JGR Space Physics

RESEARCH ARTICLE
10.1029/2020JA028989

Key Points:
- We found a preconditioning effect on the temporal evolution of X-mode ion gyro-harmonic structures observed far away from the Heating facility
- X-mode ion gyro-harmonic spectral structures and field-aligned artificial irregularities coexist during high frequency (HF) pumping below electron gyro-harmonics
- Electron accelerations along and across the magnetic field coexist during X-mode HF pumping at frequencies below electron gyro-harmonics

Correspondence to:
N. F. Blagoveshchenskaya,
nataly@aari.nw.ru

Citation:
Kalishin, A. S., Blagoveshchenskaya, N. F., Borisova, T. D., & Yeoman, T. K. (2021). Ion gyro-harmonic structures in stimulated emission excited by X-mode high power HF radio waves at EISCAT. *Journal of Geophysical Research: Space Physics*, *126*, e2020JA028989. https://doi.org/10.1029/2020JA028989

Received 30 NOV 2020
Accepted 22 JUL 2021

Ion Gyro-Harmonic Structures in Stimulated Emission Excited by X-Mode High Power HF Radio Waves at EISCAT

A. S. Kalishin[1], N. F. Blagoveshchenskaya[1], T. D. Borisova[1], and T. K. Yeoman[2]

[1]Arctic and Antarctic Research Institute, St. Petersburg, Russia, [2]University of Leicester, School of Physics and Astronomy, Leicester, UK

Abstract The distinctive features of the ion gyro-harmonic discrete structures in the narrowband stimulated electromagnetic emission (NSEE) spectra (within ±1 kHz of the heater frequency), excited by an extraordinary (X-mode) polarized high frequency (HF) pump wave in the *F*-region of the high latitude ionosphere, are reported. Results were obtained from three sets of experiments at the EISCAT (European incoherent Scatter) HF Heating facility at pump frequencies of 5.423, 6.77 and 7.953 MHz, which are below the fourth, fifth, and sixth electron gyro-harmonics. High power HF radio waves were radiated in the magnetic field-aligned direction with an effective radiated power of 238–740 MW. Discrete spectral features, ordered by the ion gyro frequency (for O^+ ions), were recorded at a large distance (1,200 km) away from the Heating facility. Up to 10 downshifted discrete ion gyro-harmonic structures paired with the upshifted spectral components (Stokes and anti-Stokes modes) in the NSEE spectra have been excited in the course of these experiments. It was found that preconditioning effects have a significant impact on the temporal evolution of the discrete spectral structures. The ion gyro-harmonic structures coexisted with field-aligned artificial irregularities (FAIs). Comparing the NSEE and EISCAT incoherent scatter radar observational results, it was concluded that the electron accelerations along and across the geomagnetic field coexist during X-mode heating. The magnetized stimulated Brillouin scatter and stimulated ion Bernstein scatter are discussed as relevant processes for the observed multiple down- and upshifted ion gyro-harmonic structures in the NSEE spectra.

Plain Language Summary Experiments in the Earth's ionosphere (part of the upper atmosphere) using high power high frequency (HF, or shortwave) radio waves may be used to study a wide variety of fundamental phenomena. We discuss recent advances in observations of stimulated radio emissions generated by a powerful HF radio transmitter at the European incoherent Scatter observatory in northern Norway. We found that the high power HF wave is able to generate radio emissions that can be observed more than one thousand kilometers away, in Saint Petersburg, Russia. We found and investigated distinctive frequencies of the radio emissions, and we believe, based on past results, that such emissions are not observable from locations close to the radio transmitter. The emissions we observed can be exploited for diagnostics of the Earth's environment, and they are similar to emissions seen in laser interactions with ionized gases such as occur in laser fusion experiments, and also in piezoelectric semiconductor devices, in fiber optics, and in many biological systems. This opens a window for utilizing our results to assist in these and other related areas.

1. Introduction

One of the most prominent phenomena discovered from ionosphere modification experiments is the stimulated electromagnetic emission (SEE) generated by the ordinary (O-mode) polarized high power high frequency (HF) radio waves (Thidé et al., 1982). A large number of SEE studies at different HF Heating facilities located at high and middle latitudes have been summarized by Leyser (2001). The SEE spectra provide important diagnostic information about the ionosphere. Various spectral components in the SEE spectra have been observed in the frequency band of 200 kHz around the heater frequency. This is the so-called wideband stimulated electromagnetic emission (WSEE).

By a contrast to the "classic" WSEE, new intense spectral components within ±1 kHz of the heater frequency were recently found at the High Frequency Active Auroral Research Program (HAARP) facility.

That artificial emission was named as the narrowband stimulated electromagnetic emission (NSEE). It was shown that an O-mode HF pump wave may decay into an electrostatic plasma wave and scattered electromagnetic (EM) waves involved in the process of Magnetized Stimulated Brillouin Scatter (MSBS) (Bernhardt et al., 2009, 2010; Mahmoudian, Scales, Bernhardt, Fu, et al., 2013; Norin et al., 2009). Excited electrostatic waves in the ionosphere source region could be either ion-acoustic (IA) or electrostatic ion cyclotron (EIC) waves, depending on the angle between the wave vector and the background magnetic field vector *B*. IA waves were excited in the interaction region along the magnetic field *B* and the EIC waves were dominant nearly perpendicular to *B*, that is consistent with the theoretical predictions (Bernhardt et al., 2010; Shukla & Stenflo, 2010). European incoherent Scatter (EISCAT) O-mode HF pumping experiments with frequency stepping through the third $3f_{ce}$ and fourth $4f_{ce}$ electron gyro-harmonics (Borisova et al., 2014; H. Y. Fu et al., 2020) have demonstrated that MSBS IA lines were excited above and below electron gyro-harmonics and suppressed as the pump frequency approached close to $3f_{ce}$ and $4f_{ce}$. NSEE spectra, recorded at pump frequencies in the vicinity of the second electron gyro-harmonic, have demonstrated the excitation of ion gyro-harmonic discrete structures ordered by the local ion gyro-frequency (for O^+ ions) (Bernhardt et al., 2011; H. Fu et al., 2013; Mahmoudian, Scales, Bernhardt, Samimi, et al., 2013; Samimi et al., 2012, 2013, 2014). The observed ion gyro-harmonic structures were downshifted relative to the pump frequency (Samimi et al, 2012, 2013). According to the analytical model (Samimi et al., 2014), these discrete structures, so-called stimulated ion Bernstein scatter (SIBS), are excited due to the parametric decay of the pump field into an UH/ EB wave and neutralized ion Bernstein (IB) modes. As shown by Mahmoudian, Scales, Bernhardt, Samimi, et al. (2013), the SIBS feature has been observed simultaneously with the HF-induced optical emission. Ion gyro-harmonic structures excited near the second electron gyro-harmonic may be able to play an important role in the creation of artificial ionization layers and potential applications (Mishin et al., 2016; Pedersen et al., 2010, 2011).

As a rule, for modification of the upper ionosphere (*F* region) the ordinary polarized (O-mode) HF pump waves are used. At HAARP the NSEE structures were only observed in the close vicinity of HF heater and only with O-mode HF transmissions. In none of the HAARP experiments, all with observations carried out in the vicinity of the HF heater, were IA and EIC emission lines observed to be excited by X-mode HF pump waves (Mahmoudian, Scales, Bernhardt, Fu, et al., 2013; Mahmoudian et al., 2014). At Sura heating facility (near N. Novgorod, Russia) observations of NSEE were not carried out at all. The nonlinear plasma processes, induced by extraodinary (X-mode) polarized HF pump wave, producing NSEE remain not well investigated and understood.

In early HF heating experiments at the EISCAT scientific association site Thidé et al. (1983) observed narrow peaks ordered by the ion gyro-frequency at about 50 Hz in the NSEE spectrum that formed banded, upshifted structures relative to the pump frequency. These structures were recorded in the neighborhood of the HF Heating facility at Tromsø, when the extraordinary polarized (X-mode) HF pump wave was vertically radiated at frequency in the vicinity of the local second electron gyro-harmonic frequency (f_H = 2.759 MHz). However, the authors of this article could not "exclude instrumental effects" for these observations. In order to explain the observed spectral structures Sharma et al. (1994) have proposed the parametric decay instability of an X-mode HF pump wave into a high-frequency electron Bernstein wave and a low-frequency ion Bernstein wave.

Recent experiments at EISCAT have demonstrated for the first time that an X-mode HF pump wave is capable of exciting the NSEE (within ±1 kHz off the pump frequency) recorded at 1,200 km away from the Heating facility (Blagoveshchenskaya et al., 2015). Intense spectral structures associated with EIC, and multiple harmonics of EIC have been found in the NSEE spectra (Blagoveshchenskaya et al., 2015). It was suggested that the parametric decay of the extraordinary polarized high power electromagnetic wave into the electron Bernstein and ion Bernstein plasma waves is responsible for the observed discrete spectral structures ordered by the local ion gyro-frequency (O^+ ions). We have focused our attention on results obtained in the course of X-mode frequency stepping over the fifth electron gyro-harmonic (Blagoveshchenskaya et al., 2017). It was shown that the disappearance of the ion gyro-harmonic structures in the NSEE spectra occurred when the heater frequency reached the fifth electron gyro-harmonic frequency. This feature can provide a long distance determination of the local electron gyro-frequency over the Heating facility. The multiple down- and upshifted ion gyro-harmonic structures did not reappear within about 150 kHz range above the electron gyro-harmonic frequency (Blagoveshchenskaya et al., 2017).

Field-aligned artificial irregularities (FAIs) play a key role for the NSEE observations on the ground. As for small-scale field-aligned irregularities induced by the ordinary (O-mode) polarized powerful HF radio waves (HF pump wave), they are intensively studied at all HF heating facilities in the world (see, for example, Gurevich, 2007; Robinson, 1989 and references therein). They are generated at the upper hybrid resonance height, which is several kilometers below the reflection altitude of the HF pump wave, through the thermal parametric (resonance) instability (Grach & Trakhtengerts, 1975; Vas'kov & Gurevich, 1976). Investigations of FAIs induced by extraordinary (X-mode) HF pump waves in the high latitude ionosphere *F*-region have been carried out during a large number of EISCAT HF pumping experiments (Blagoveshchenskaya, 2020; Blagoveshchenskaya et al., 2011, 2015, 2017, 2019, 2020). The features and behavior of the X-mode FAIs differ radically from O-mode effects. The X-mode FAIs, similar to the other X-mode phenomena, were only excited by HF pump waves radiated toward the magnetic zenith (Blagoveshchenskaya et al., 2015). They were excited at pump frequencies below and above the critical frequency of the *F*2 layer ($f_H \leq foF2$ and $f_H > foF2$) (Blagoveshchenskaya, 2020; Blagoveshchenskaya et al., 2011, 2015, 2019). The generation of the X-mode FAIs occurs in two steps. At first the large scale field-aligned irregularities ($l_\perp$ = 1–10 km) were excited, and then large-scale structures collapsed into the small-scale sizes (Blagoveshchenskaya et al., 2019).

The aim of the current study is to provide insight into new issues associated with the ion gyro-harmonic structures excited by an X-mode HF pump wave in the *F*-region of the high latitude ionosphere and observed far away from the EISCAT/Heating facility (about 1,200 km). We report experimental results regarding the distinctive features and behaviors of the ion gyro-harmonic discrete structures in the NSEE spectra within ± 1 kHz off the pump frequency at pump frequencies below the fourth, fifth and sixth electron gyro-harmonics. Alternating O- and X-mode experiments were carried out under quiet geophysical conditions in the sunlight ionosphere. HF pumping was made into the magnetic zenith at different pump frequencies below the critical frequency of the *F*2 layer. This makes it possible to compare the X- and O-mode effects in the same geophysical conditions and heater details.

The study is organized as follows. Experimental setup is described in Section 2. Next, we present the experimental results concerning the distinctive features of the ion gyro-harmonic structures excited by an X-mode HF pump wave at different frequencies below or near the critical frequency of the *F*2 layer ($f_H \leq foF2$) and observed at 1,200 km away from the EISCAT/Heating facility (Section 3). Preconditioning effects on the temporal evolution of the ion gyro-harmonic structures is considered in Section 3.1. Then, we present results related to the coexisting ion gyro-harmonic structures and small-scale artificial field-aligned irregularities (Section 3.2). Next, we have considered the impact of the ratio $f_H/ foF2$ on the ion gyro-harmonic generation (Section 3.3). Finally, a discussion and summary are provided (Section 4).

2. Experimental Setup

The modification of the high latitude ionosphere was produced by the EISCAT HF Heating facility in the vicinity of Tromsø, Norway (69.6°N, 19.2°E) (Rietveld et al., 2016). Three sets of experiments aimed toward the investigation of the NSEE in the high latitude upper (*F*-region) ionosphere were conducted in daylight hours on February 25, 2013 (Experiment 1), October 28, 2015 (Experiment 2), and October 25, 2013 (Experiment 3), which were a part of Russian EISCAT heating campaigns. High power electromagnetic waves were radiated into the magnetic zenith (HF heater beam tilted by 12°S from the vertical pointing) under quiet geophysical conditions in the sunlight ionosphere. On February 25, 2013 concurrent O- and X-mode HF pumping was made at the pump frequency of 5.423 MHz with a 10 min on, 5 min off transmission scheme. During the second set of experiments on October 28, 2015 the concurrent O- and X-mode HF pump waves were radiated at frequencies of 6.77 MHz and then 5.423 with 10 min on, 5 min off transmission pulses. In the course of the third set on October 25, 2013 only the X-mode heating was made at frequencies of 5.423, 6.2, 7.1, and 7.953 MHz with a 2.5 min on, 1 min off transmission scheme. In all experiments the pump frequency was below or near the critical frequency of the *F*2 layer ($f_H \leq foF2$) enabling a comparison between the O- and X-mode effects for the first and second set of experiments. The width of the heater beam was 5–6° (at the - 3 dB level). Effective radiated power changed between 238 and 740 MW in different experiments. The leakage of the ordinary polarized wave during the transmission of the extraordinary HF pump wave, as well as the leakage of extraordinary polarized wave in the course the O-mode HF pumping, did not exceed 5 MW.

The observations of NSEE have been carried out near St. Petersburg (60.27°N, 29.37°E) located at 1,200 km away from the Heating facility. HF heater signals were received on a double rhombic antenna directed over Tromsø. During the first set of experiments on February 25, 2013, HF signals were recorded by a SDR (Software Defined Radio) PERSEUS receiver with a dynamic range not worse than 90 dB. The fast Fourier transform was utilized to obtain spectrograms of the received signal. A frequency resolution of the power spectrum of 0.16 Hz and a temporal resolution of 3 s were used for processing data on February 25, 2013. During the second and third set of experiments on October 28, 2015, and October 25, 2013 HF heater signals were recorded by a digital spectrum-analyzer, the ICOM-R75 receiver with a 90 dB dynamic range. This allows us to obtain the spectral features in a band of 2.5 kHz. In the course of the second and third set of experiments, a frequency resolution of 0.42 Hz and a temporal resolution of 3 s were utilized.

FAIs were probed by the CUTLASS (Co-operative UK Twin Located Auroral Sounding System) HF coherent radar (Lester et al., 2004) located at Hankasalmi, Finland (62.3°N; 26.6°E). On October 28, 2015 CUTLASS run at six operational frequencies from about 10 to 20 MHz that monitored the FAI features and behaviors transverse to the magnetic field with sizes of $l_{\perp} \approx 7.5$–15 m ($l_{\perp} = c/2f$, where f is the CUTLASS operational frequency). Three CUTLASS operational frequencies of 16, 18, and 20 MHz, related to the FAI size with $l_{\perp} \approx 9.2$, 8.3, and 7.5 m, have been utilized in the course of the experiment on October 25, 2013. CUTLASS operated on a single beam 5 (beam width of ~3.3°) directed over Tromsø with a range gate of 15 km and a temporal resolution of 3 s. NSEE observations in the vicinity of St. Petersburg were also carried out simultaneously with the EISCAT UHF incoherent scatter radar (933 MHz) (Rishbeth & van Eyken, 1993) measurements at Tromsø, co-located with the HF heater. The UHF radar measured in the same direction as the pointing of the HF heater transmission. Processing EISCAT UHF radar data was done using the Grand Unified Incoherent Scatter Design and Analysis Package software (Guisdap) (Lehtinen & Huuskonen, 1996).

The status of the ionosphere above Tromsø in the course of HF pumping experiments was checked by the Tromsø dynasonde (Rietveld et al., 2008) and digisonde (Galkin et al., 2008).

3. Results of Observations

3.1. Preconditioning Effect on the Temporal Evolution of the Ion Gyro-Harmonic Structures

During the first set of experiments on February 25, 2013 an HF pump wave at $f_H = 5.423$ MHz was radiated in the magnetic field-aligned direction with a zenith angle of 12°S from 15:42 to 17:12 UT with O- and X-mode polarization by cycles 10 min on, 5 min off with the effective radiated power ERP = 416 MW. The critical frequency of the $F2$ layer was about 5.6 MHz ($f_H/foF2 = 0.97$). Experimental observations of the NSEE spectral features are summarized in Figures 1–3.

Figure 1 presents the spectrogram of the NSEE in the frequency band of ± 700 Hz of the pump frequency recorded on February 25, 2013 from 16:00 to 16:42 UT near St. Petersburg at 1,200 km far away from the EISCAT/Heating facility. The strong line in the center with zero frequency offset corresponds to the HF pump wave. As evident from Figure 1, only during the X-mode pulses (16:16–16:26 UT and 16:31–16:41 UT) are the discrete ion gyro-harmonic structures ordered by the ion gyro-frequency seen on the spectrogram, both down- and upshifted relative to the pump frequency. Weak and narrow multiple harmonics of 50 Hz, seen under the O-mode HF pumping, are power supply harmonic interference. We assume that the maximum error for the true range of the reflection altitude of the X-mode HF pump wave at $f_H = 5.423$ MHz based upon the ionosonde measurements at Tromsø does not exceed 10 km (Galkin et al., 2008). By using the International Geomagnetic Reference Field (IGRF) model at the altitudes of 230 ÷ 220 km, the electron gyro-frequency lied in the range $f_{ce} = 1.359 \div 1.365$ MHz and the ion gyro-frequency was $f_{ci} = 46.6 \div 46.8$ Hz. It corresponds that the pump frequency $f_H = 5.423$ MHz was about (13 ÷ 37) kHz below the fourth electron gyro-harmonic ($4f_{ce} = 5.436 \div 5.460$ MHz). The additional argument in support of the heater frequency below the electron gyro-harmonic is evident from recent results obtained in the course of X-mode frequency stepping over the fifth electron gyro-harmonic from below. Blagoveshchenskaya et al. (2017) have shown that the disappearance of the multiple ion gyro-harmonic structures in the NSEE spectra occurred when

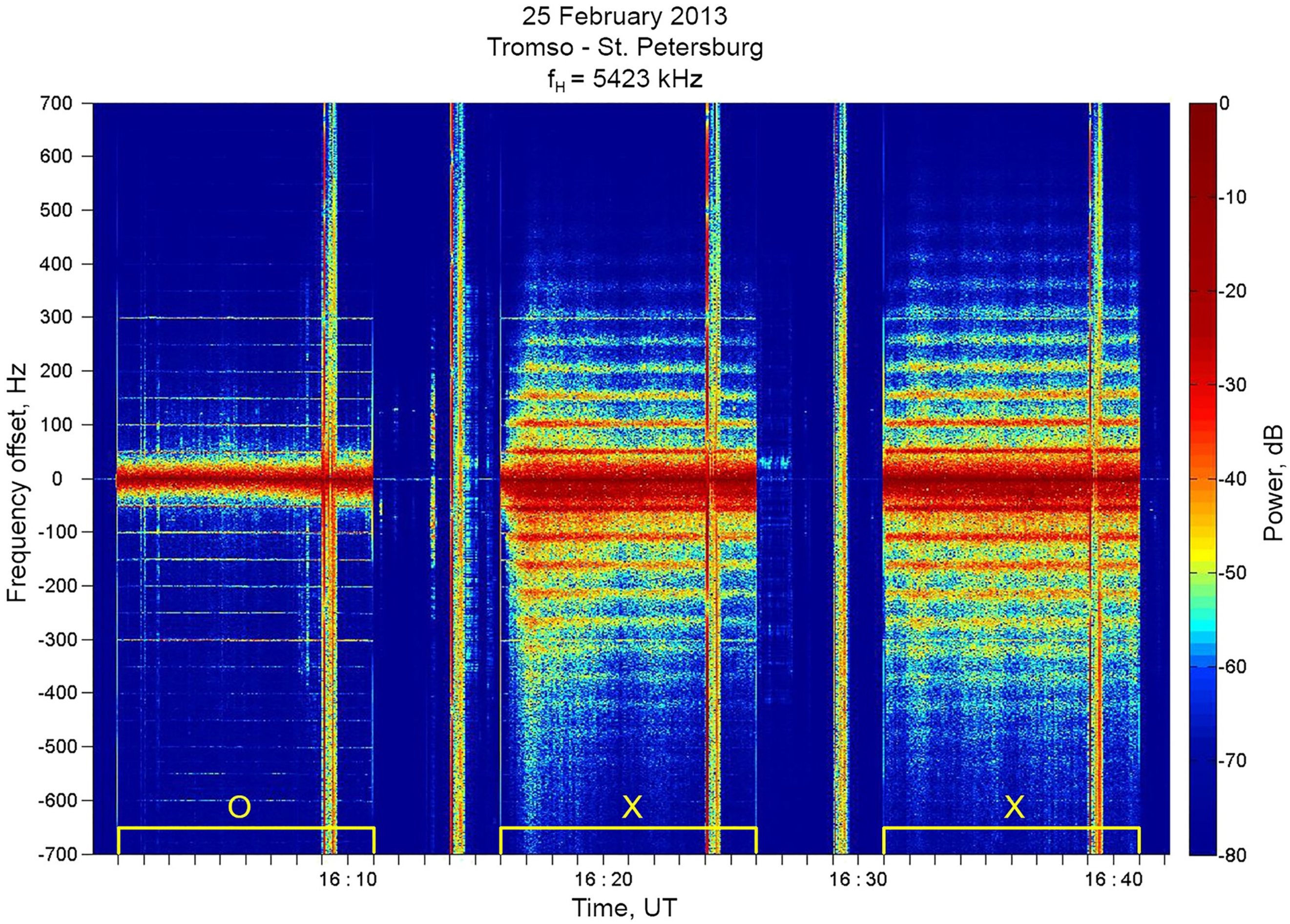

Figure 1. Experiment 1. The spectrogram of the narrowband stimulated electromagnetic emission (NSEE) at a pump frequency $f_H = 5.423$ MHz in the frequency band of ±700 Hz off the pump frequency recorded on February 25, 2013 from 16:00 to 16:42 UT near St. Petersburg at 1,200 km away the EISCAT/Heating facility. Alternating O- and X-mode high frequency (HF) pumping was made into the magnetic zenith with 10 min on, 5 min off cycles with the effective radiated power ERP = 416 MW. Weak and narrow multiple harmonics of 50 Hz, seen under the O-mode HF pumping, are power supply harmonic interference. Weak short-lived upshifted structures at about 0.5 f_{ci}, appearing and disappearing before and after the pump cycle from 16:16 to 16:26 UT, are interference. The pump pulses and polarization of the heater wave are shown on the time axis.

the heater frequency reached the electron gyro-harmonic frequency. The multiple down- and upshifted ion gyro-harmonic structures did not re-appear within about 150 kHz band above the electron gyro-harmonic frequency. Thus, the presence of multiple down- and upshifted ion gyro-harmonic structures in the NSEE spectra indicate that the heater frequency is below the electron gyro-harmonics.

The downshifted (Stokes) spectral lines were paired with upshifted (anti-Stokes) spectral lines. Eleven down- and nine upshifted discrete spectral lines ordered by approximately the ion gyro-frequency (O^+ ions) are clearly identified in spectrogram during the X-mode HF pump pulses. Among the ion gyro-harmonic structures with the maximum spectral power at (nf_{ci}), where n is the harmonic number, the downshifted spectral line at $0.5f_{ci}$ was also excited. In the course of the O-mode cycle from 16:01–16:11 UT, the discrete spectral structures did not occur. Only very weak and narrow power supply harmonic interference at multiples of 50 Hz can be seen during the O-mode transmission pulse.

The comparison between the temporal evolution of the X-mode pulse from the "cold" start (the first X-mode pulse from 16:16–16:26 UT following the O-mode one) and the second X-mode cycle (16:31–16:41 UT) exhibit distinctions. It is clearly seen that from the "cold" start all spectral lines do not start to develop at the same time. With increasing harmonic number, the delay time from the heater turning on becomes longer,

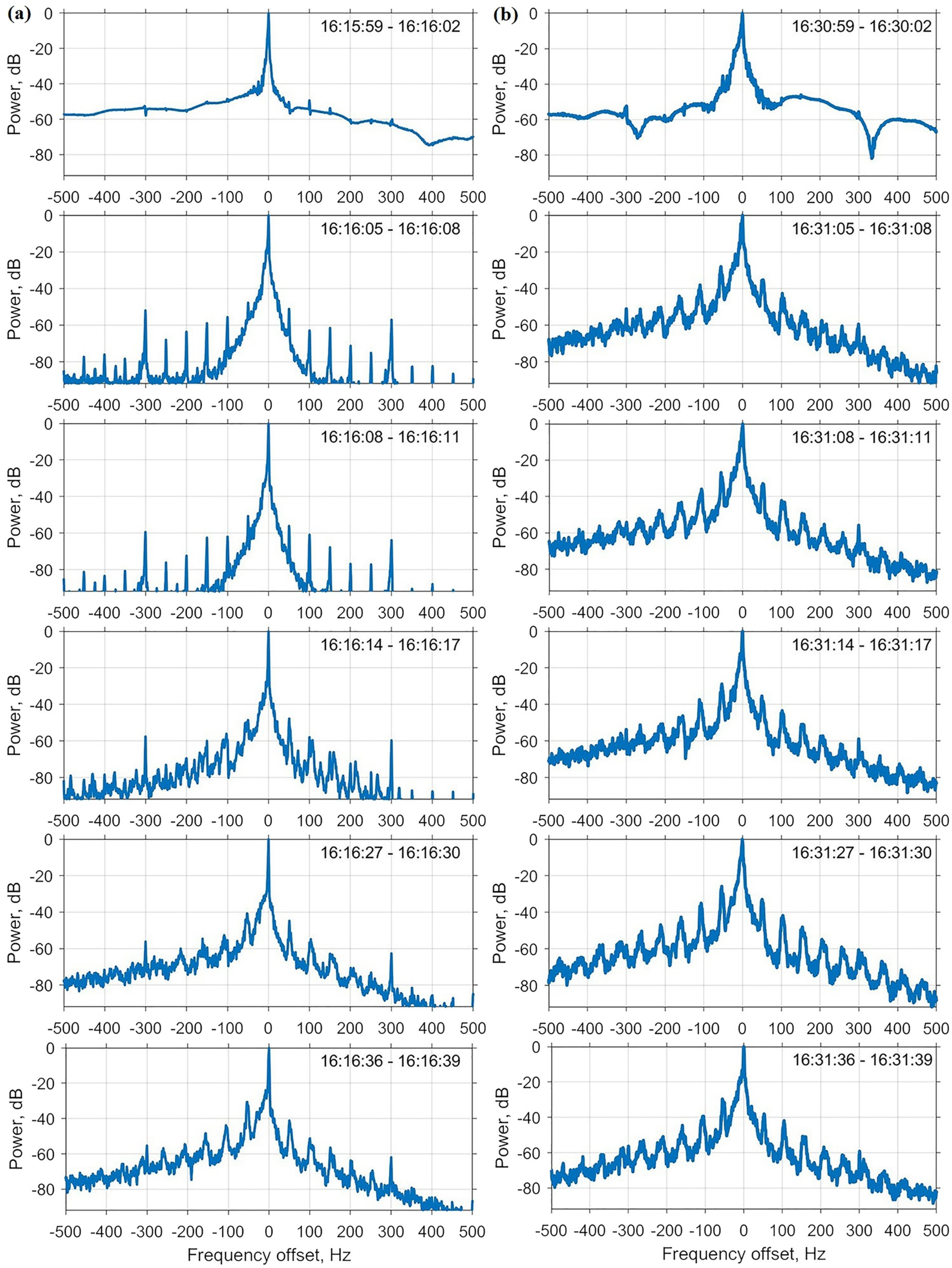

Figure 2. Experiment 1. The power spectra of narrowband stimulated electromagnetic emission (NSEE) obtained on February 25, 2013 at $f_H = 5.423$ MHz in the frequency band of ±500 Hz taken over 3 s intervals for first 40 s after the high frequency (HF) heater is turned on. (a) Power spectra from the "cold" start from 16:16 to 16:26 UT. (b) Power spectra in the following X-mode pulse from 16:31 to 16:41 UT. Weak and narrow power supply harmonic interference at multiples of 50 Hz are seen in spectra from the "cold" start at 16:16:05–16:16:08 and 16:16:08–16:16:11 UT. The heater details are the same as in Figure 1.

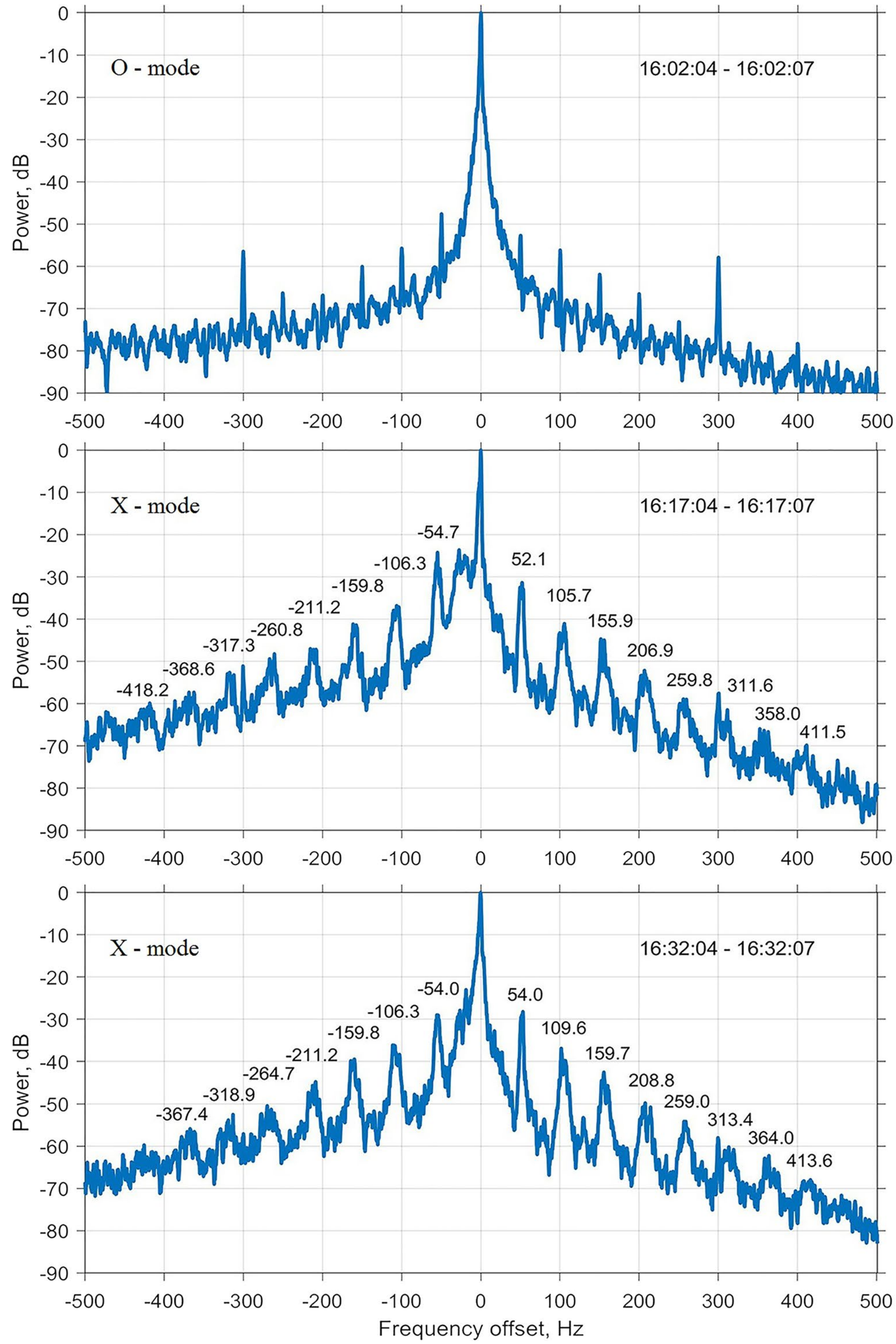

Figure 3. Experiment 1. Power spectra of narrowband stimulated electromagnetic emission (NSEE) on February 25, 2013 at $f_H = 5.423$ MHz taken over 3 s intervals after about one minute of the pumping process for the O-mode pulse at 16:02:04–16:02:07 UT and for the X-mode pulses at 16:17:04–16:17:07 UT and 16:32:04–16:32:07 UT. The spectrum for the O-mode pulse exhibits only weak and narrow multiple harmonics of the 50 Hz power supply. Digits on the X-mode spectra indicate the frequency offsets of the observed downshifted and upshifted spectral maxima which are close to the harmonics of the ion gyro-frequency for O^+ ions. The heater details are the same as in Figure 1.

the spectral line power decreases, and the spectral bandwidth grows, which implies a nonlinear cascading process.

Let's consider in more detail and compare the NSEE spectra recorded near St. Petersburg in the course of two consecutive X-mode heater pulses in which the first one is from the "cold" start. Figure 2 demonstrates the power spectra in a frequency band of ±500 Hz taken over 3 s intervals during first 40 s after the HF heater is turned on. Figures 2a and 2b present the spectra recorded from the "cold" start during the heater pulse from 16:16–16:26 UT and in the following X-mode pulse from 16:31–16:41 UT, respectively. As seen from Figure 2a ion gyro-harmonic structures start to develop after ~15 s (in the 3 s interval 16:16:14–16:16:17 UT), while in the following X-mode cycle (see Figure 2b) they develop faster, about ~6 s from the HF pump onset (in the 3 s interval 16:31:05–16:31:08 UT). Weak and narrow harmonics of the 50 Hz power supply are seen in the spectra of Figure 2a before 16:16:14 UT. Thus, the results obtained clearly demonstrate the preconditioning effects on the temporal evolution of the ion gyro-harmonic structures, induced by X-mode HF pumping.

Figure 3 illustrates spectra taken over 3 s intervals showing the discrete ion gyro-harmonic structures obtained after about one minute of the X-mode heating process at 16:17:04–16:17:07 UT and 16:32:04–16:32:07 UT in the course of the abovementioned pump pulses. For the comparison we also present the O-mode spectrum at 16:02:04–16:02:07 UT. It is evident from Figure 3 that both X-mode spectra are very similar after 1 min of the heating process. The power of the spectral maxima drops by 30 dB for the downshifted sideband and by 40 dB for the upshifted one from the first to the 8th harmonic of the ion gyro-frequency. In the same conditions the spectral width of discrete structures increased from 20 to 50 Hz. The O-mode spectrum at 16:02:04–16:02:07 UT exhibits only very narrow and weak multiple harmonics of the 50 Hz power supply.

3.2. Coexisting Ion Gyro-Harmonic Structures and Small-Scale Artificial Field-Aligned Irregularities

In the course of the second set of experiments, the NSEE measurements were accompanied by CUTLASS observations. The experiment was carried out on October 28, 2015, in which the pump pulse was 10 min on, 5 min off. Alternating X-/O-mode heating was carried out at pump frequency $f_H = 6.77$ MHz from 14:16 to 14:41 UT with an effective radiated power ERP = 480 MW. The critical frequency of the $F2$ layer was about was about 6.8 MHz ($f_H/ foF2 = 0.99$). Then from 15:31 to 15:56 UT the alternating O-/X-mode heating was produced at $f_H = 5.423$ MHz with an effective radiated power ERP = 238 MW. In this event the value of $foF2$ was estimated to be about 5.5 MHz ($f_H/ foF2 = 0.99$).

We assume that the maximum error for the true range of the reflection altitude of the X-mode HF pump wave at $f_H = 6.77$ MHz based upon the ionosonde measurements does not exceed 10 km (Galkin et al., 2008). From the IGRF model at the altitudes 230 ÷ 220 km the electron gyro-frequency changed in the range $f_{ce} = 1.359 \div 1.365$ MHz and the ion gyro-frequency was $f_{ci} = 46.6 \div 46.8$ Hz. It corresponds that the pump frequency $f_H = 6.77$ MHz was about (25 ÷ 55) kHz below the fifth electron gyro-harmonic ($5f_{ce} = 6.795 \div 6.825$ MHz). The HF pump wave at $f_H = 5.423$ MHz was reflected at altitude between 225 and 215 km. From the IGRF model at these altitudes the electron gyro-frequency changed from $f_{ce} = 1.362 \div 1.367$ MHz and the ion gyro-frequency was $f_{ci} = 46.7 \div 46.8$ Hz. It corresponds that the pump frequency $f_H = 5.423$ MHz was about (25 ÷ 45) kHz below the fourth electron gyro-harmonic ($4f_{ce} = 5.448 \div 5.468$ MHz).

The spectrogram of the NSEE in the frequency band of ±250 Hz off the pump frequency obtained near St. Petersburg on October 28, 2015 from 14:12 to 14:42 UT ($f_H = 6.77$ MHz) and from 15:28–15:58 UT ($f_H = 5.423$ MHz) is shown in Figure 4. Spectra demonstrating the ion gyro-harmonic structures at $f_H = 6.77$ MHz and $f_H = 5.423$ MHz are depicted in Figures 5 and 6 respectively. To consider the spectra in detail, Figures 4–6 illustrate only the first four harmonics, which were the most intense, while the number of detectable harmonics reached $n = 8$–9. Similar to the experiment on February 25, 2013, in the course of X-mode HF pumping at $f_H = 6.77$ MHz and $f_H = 5.423$ MHz on October 28, 2015, down- and upshifted discrete ion harmonic structures ordered by the ion gyro-frequency were also generated. Again, among with the spectral lines with the maximum at nf_{ci}, the downshifted spectral line at $0.5f_{ci}$ and occasionally even at $1.5f_{ci}$ were also generated.

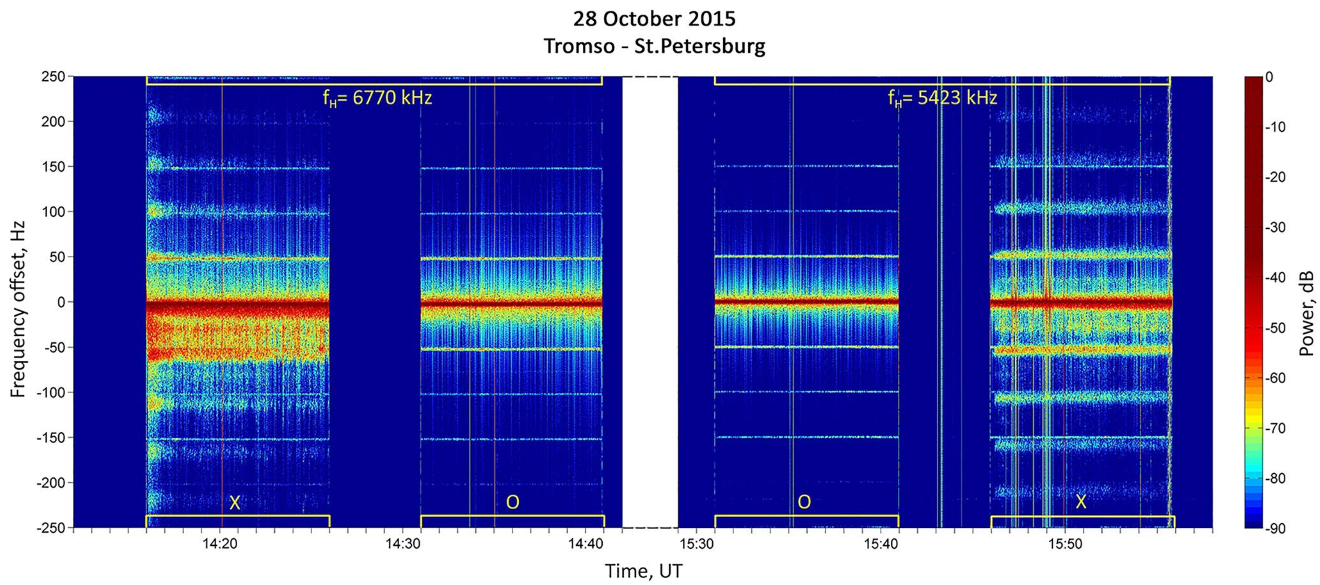

Figure 4. Experiment 2. The spectrogram of the narrowband stimulated electromagnetic emission (NSEE) on October 28, 2015 in the frequency band of ±250 Hz off the pump frequency obtained near St. Petersburg at 1,200 km away from the EISCAT/Heating facility when high frequency (HF) pump wave was radiated into the magnetic zenith with 10 min on, 5 min off cycles. From 14:12 to 14:42 UT HF pumping was produced at frequency of f_H = 6.77 MHz with an effective radiated ERP = 480 MW and from 15:28–15:58 UT at f_H = 5.423 MHz with ERP = 238 MW. The pump pulses and polarization of heater wave are shown on the time axis. Weak and narrow multiple harmonics of 50 Hz are power supply harmonic interference. The pump pulses and polarization of the heater wave are shown on the time axis.

The NSEE observations near St. Petersburg were accompanied by a CUTLASS radar run at Hankasalmi (Finland), which was operating the only beam (beam 5) oriented over Tromsø. Details of the CUTLASS measurements are the same as given by Blagoveshchenskaya et al. (2014). CUTLASS run almost simultaneously at six frequencies in the range of about 10–20 MHz and was sensitive to FAIs with a size of $l_\perp$ ≈7.5–15 m transverse to the magnetic field. Figures 7a and 7b depict the backscatter power at the CUTLASS operational frequencies of 10, 11.5, 13.2, 16, 18, and 20 MHz on October 28, 2015 from 14:12–14:42 UT (under HF pumping at f_H = 6.77 MHz) and from 15:28–15:53 UT at f_H = 5.423 MHz respectively. As seen from Figure 7a, at f_H = 6.77 MHz the backscatter from FAIs occurred at frequencies of 11.5, 13.2, 16.2, 18, and 20 MHz that corresponds to the FAI transverse size of $l_\perp \approx$ 13, 11.3, 9.2, 8.3, and 7.5 m. The most intense backscatter from the X-mode FAIs was observed at 18 MHz ($l_\perp \approx$ 8.3 m), while under the O-mode HF pumping the backscatter was maximized at 20 MHz ($l_\perp \approx$ 7.5 m). HF heating process at f_H = 5.423 MHz was also accompanied by the FAI generation (see Figure 7b). The strongest FAIs appeared at 16 and 18 MHz ($l_\perp \approx$ 9.2 m and $l_\perp \approx$ 8.3 m) for the X- and O-mode heating respectively. The spatial scale of artificially disturbed region in the north-south direction occupied by FAIs peaked at about of 90 and 120 km for f_H = 6.77 and f_H = 5.423 MHz respectively.

3.3. The Impact of the Ratio f_H/ $foF2$ on the Ion Gyro-Harmonic Generation

The first two sets of experiments were carried out at pump frequencies just below the critical frequency of the F2 layer (f_H/ $foF2$ = 0.97–0.99) and lying below the fourth and fifth electron gyro-harmonics. In the course of the third set of experiments on October 25, 2013 an extraordinary (X-mode) polarized HF pump wave radiated from 13:16 UT at frequencies of 5.423, 6.2, 7.1, and 7.953 MHz with effective radiated powers ERP = 416, 548, 615, and 740 MW, respectively, with a 2.5 min on, 1 min off transmission pulse. In the course of the experiment the critical frequency of the $F2$ layer was estimated to be about $foF2$ = 9.8 MHz from the dynasonde measurements at Tromsø. In such a case the ratio of f_H/ $foF2$ was significantly less than in the first two sets of experiments and estimated as f_H/ $foF2$ = 0.55; 0.63; 0.71; 0.81 for corresponding pump frequencies of 5.423, 6.2, 7.1, and 7.953 MHz.

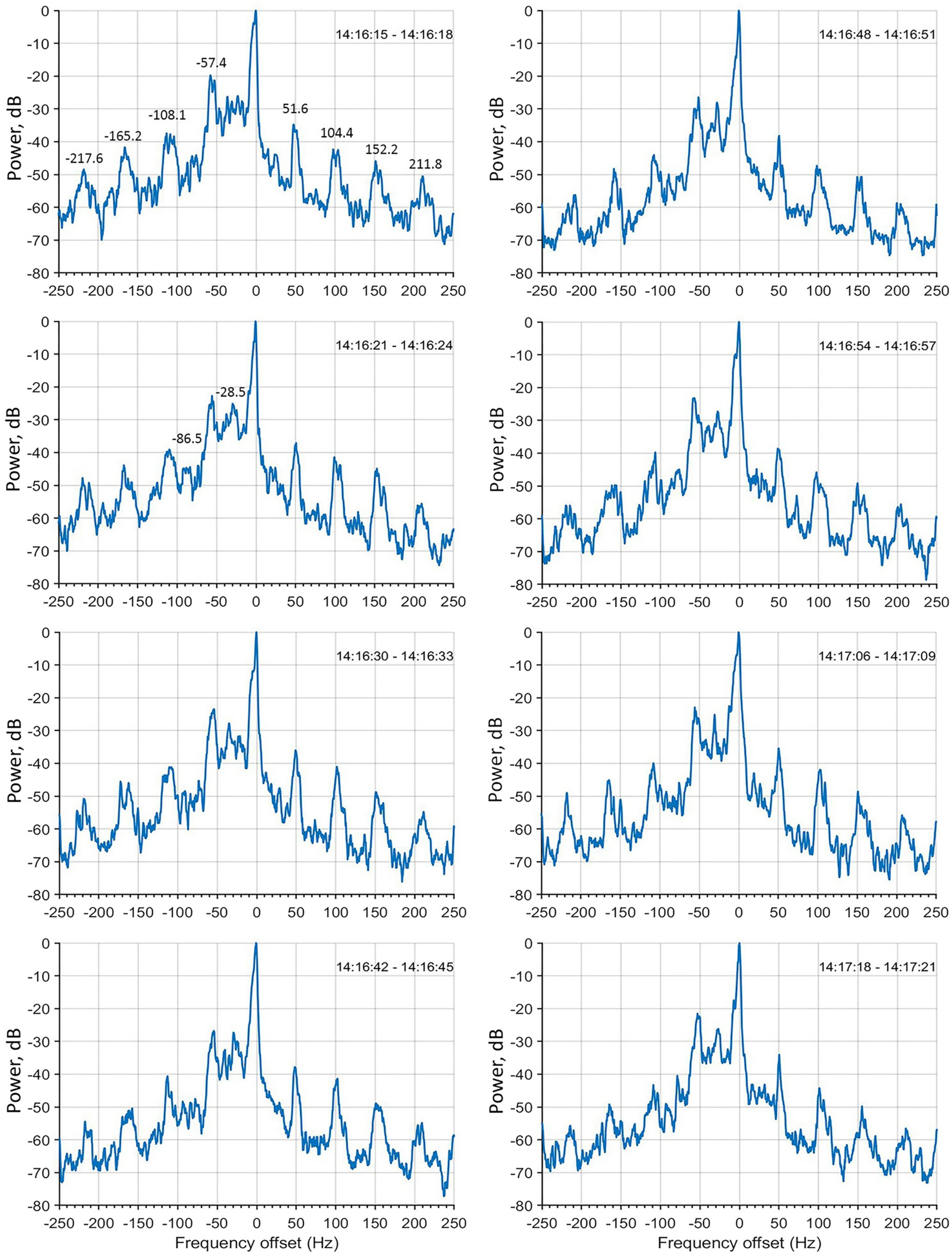
14:16:15 - 14:16:18
-217.6
-165.2
-108.1
-57.4
51.6
104.4
152.2
211.8
14:16:48 - 14:16:51
14:16:21 - 14:16:24
-86.5
-28.5
14:16:54 - 14:16:57
14:16:30 - 14:16:33
14:17:06 - 14:17:09
14:16:42 - 14:16:45
14:17:18 - 14:17:21
Power, dB
Frequency offset (Hz)

Figure 5.

Figure 8 shows the spectrogram of the NSEE in the frequency band ±250 Hz of the pump frequency taken on October 25, 2013 from 13:15 to 13:30 UT at a distance 1,200 km away from the EISCAT/Heating facility. As seen, only at f_H = 7.953 MHz did the discrete ion gyro-harmonic structures ordered by the ion gyro-frequency occur. The downshifted (Stokes) spectral lines were paired with upshifted (anti-Stokes) spectral lines.

The reflection altitude of the HF pump wave at f_H = 7.953 MHz was between 222 ÷ 212 km assuming that the maximum error for the true range of the reflection altitude does not exceed 10 km(Galkin et al., 2008). From the IGRF model at the altitudes from 222 ÷ 212 km the electron gyro-frequency changed in the range f_{ce} = 1.364 ÷ 1.369 MHz and the ion gyro-frequency was f_{ci} = 46.7 ÷ 46.9 Hz. It corresponds that the pump frequency f_H = 7.953 MHz was about (230 ÷ 260) kHz below the sixth electron gyro-harmonic ($6f_{ce}$ = 8.184 ÷ 8.214 MHz).

In parallel with the spectral lines maximized at nf_{ci}, where n is the harmonic number, the downshifted spectral lines at $0.5f_{ci}$ and $1.5f_{ci}$ were also generated. Figure 9 presents the NSEE spectra taken over 3 s intervals showing the discrete ion gyro-harmonic structures recorded at f_H = 7.953 MHz. As a whole, the NSEE spectra observed at the pump frequencies below the fourth, fifth and sixth electron gyro-harmonics are very similar.

The backscatter power at the CUTLASS operational frequencies of 16, 18, and 20 MHz, corresponding to the X-mode FAI size across the geomagnetic field of 9.2, 8.3, and 7.5 m, on October 25, 2013 from 13:15–13:30 UT is shown in Figure 10. The X-mode FAIs were generated throughout the experiment in four consecutive pump pulses, when the HF heater frequencies were changed in the sequence of 5.423, 6.2, 7.1, and 7.953 MHz, The strongest backscatter was observed at 18 MHz ($l_\perp \approx$ 8.3 m). Nonetheless, the backscatter from FAIs was much weaker as compared with February 25, 2013 and October 28, 2015. The spatial size of artificially disturbed region occupied by FAIs at any pump frequency did not exceed 30 km, that is much less than in the first two sets of experiments. The ion gyro-harmonic structures were not excited at pump frequencies of 7.1 MHz, lying above the $5f_{ce}$, and at 6.2 MHz, which is away from the nf_{ce} (see Figure 8). Because of that one would expect that under X-mode heating the ion-gyro-harmonic structures are only excited below electron gyro-harmonics ($f_H < nf_{ce}$). However, on October 25, 2013 these structures were not excited at f_H = 5.423 MHz, which was certainly lying below $4f_{ce}$, despite them being observed in the first two sets of experiments at the same pump frequency and effective radiated power. The most likely significant difference between the experiments at f_H = 5.423 MHz is the ratio of the pump frequency to the critical frequency of the F2 layer ($f_H/ foF2$ = 0.97–0.99 in the first two sets of experiments and $f_H/ foF2$ = 0.55 in the third one). Moreover, the experiment on October 25, 2013 was conducted in earlier daytime hours when the absorption is higher than in the evening hours.

4. Discussion and Summary

We would like to emphasize that strong and unexpected phenomena induced by an X-mode wave in the high latitude ionospheric *F*-region were only excited when HF pumping was directed in the magnetic field-aligned direction (magnetic zenith, MZ). By contrast to the O-mode, there were not any X-mode effects in the course of HF pumping in the vertical direction (see, for example, Blagoveshchenskaya, 2020; Blagoveshchenskaya et al., 2014, 2015). Observational results reported in this study have clearly demonstrated that an X-mode HF pumping into the magnetic zenith at frequencies lying below the fourth, fifth and sixth electron gyro-harmonics by 13–260 kHz leads to the excitation of discrete components in the NSEE spectra within a ±1 kHz frequency band around the pump frequency. The ratio of the pump frequency to the critical frequency of the F2 layer was lying in the range $f_H/ foF2$ = 0.81–0.99. An alternating O-/X-mode HF pumping during two consecutive pump pulses makes it evident that discrete structures in the NSEE spectra,

Figure 5. Experiment 2. The power spectra of narrowband stimulated electromagnetic emission (NSEE) on October 28, 2015 at f_H = 6.77 MHz in the frequency band of ±250 Hz taken over 3 s intervals in the course of the X-mode pulse from 14:16 to 14:26 UT. Digits on the X-mode spectrum taken at 14:16:15–14:16:18 UT indicate the frequency offsets of the observed downshifted and upshifted spectral maxima which are close to the harmonics of the ion gyro-frequency for O^+ ions. There are also spectral maxima, mostly pronounced in the downshifted sideband, corresponding to the values of 0.5 f_{ci} and even 1.5 f_{ci} for O^+ ions (see spectrum taken at 14:16:21–14:16: 24 UT). Such spectral maxima correspond approximately to the ion gyro-frequency for NO^+ ions and its third harmonic. The heater details are the same as in Figure 4.

10.1029/2020JA028989

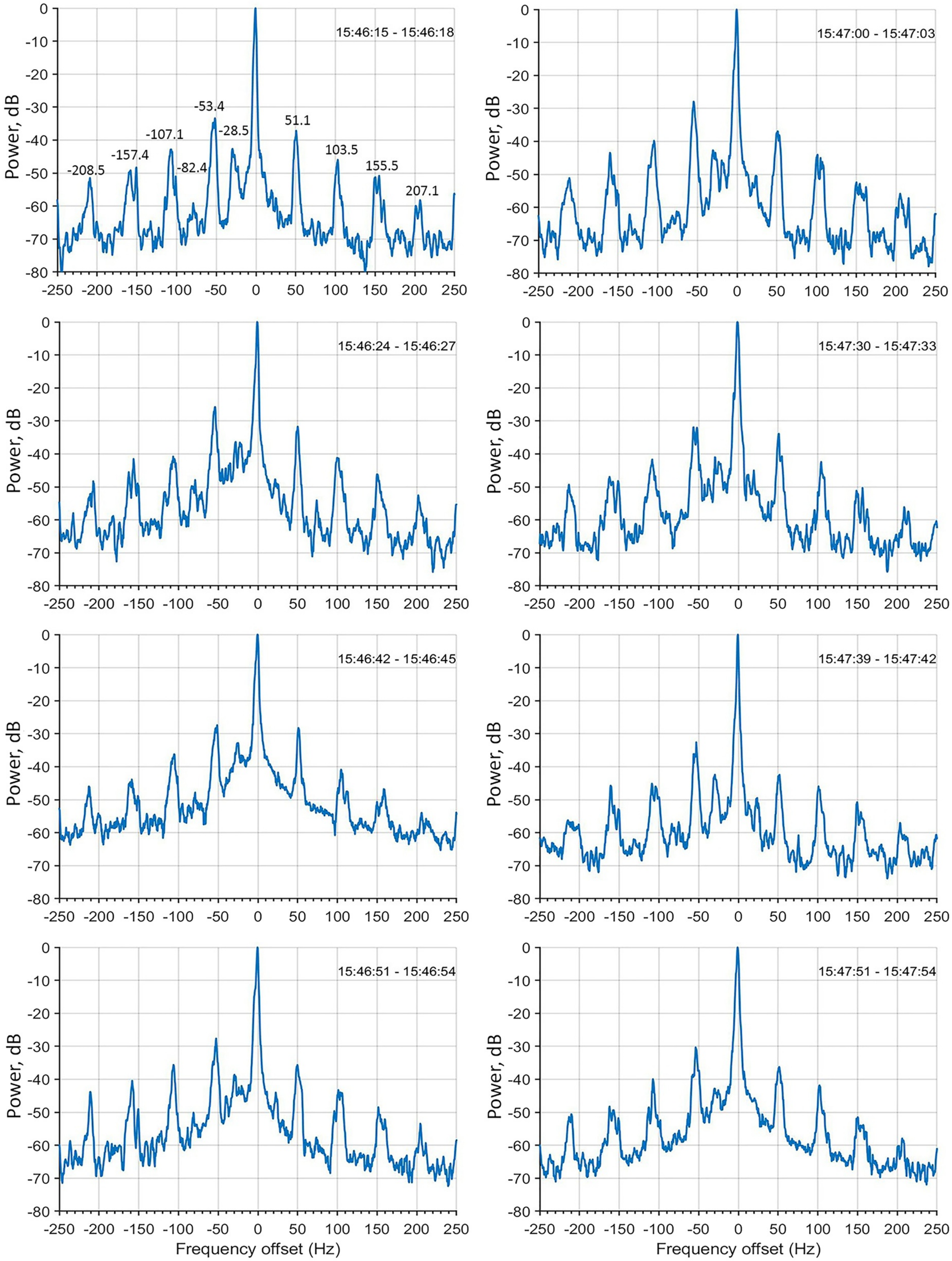

Figure 6.

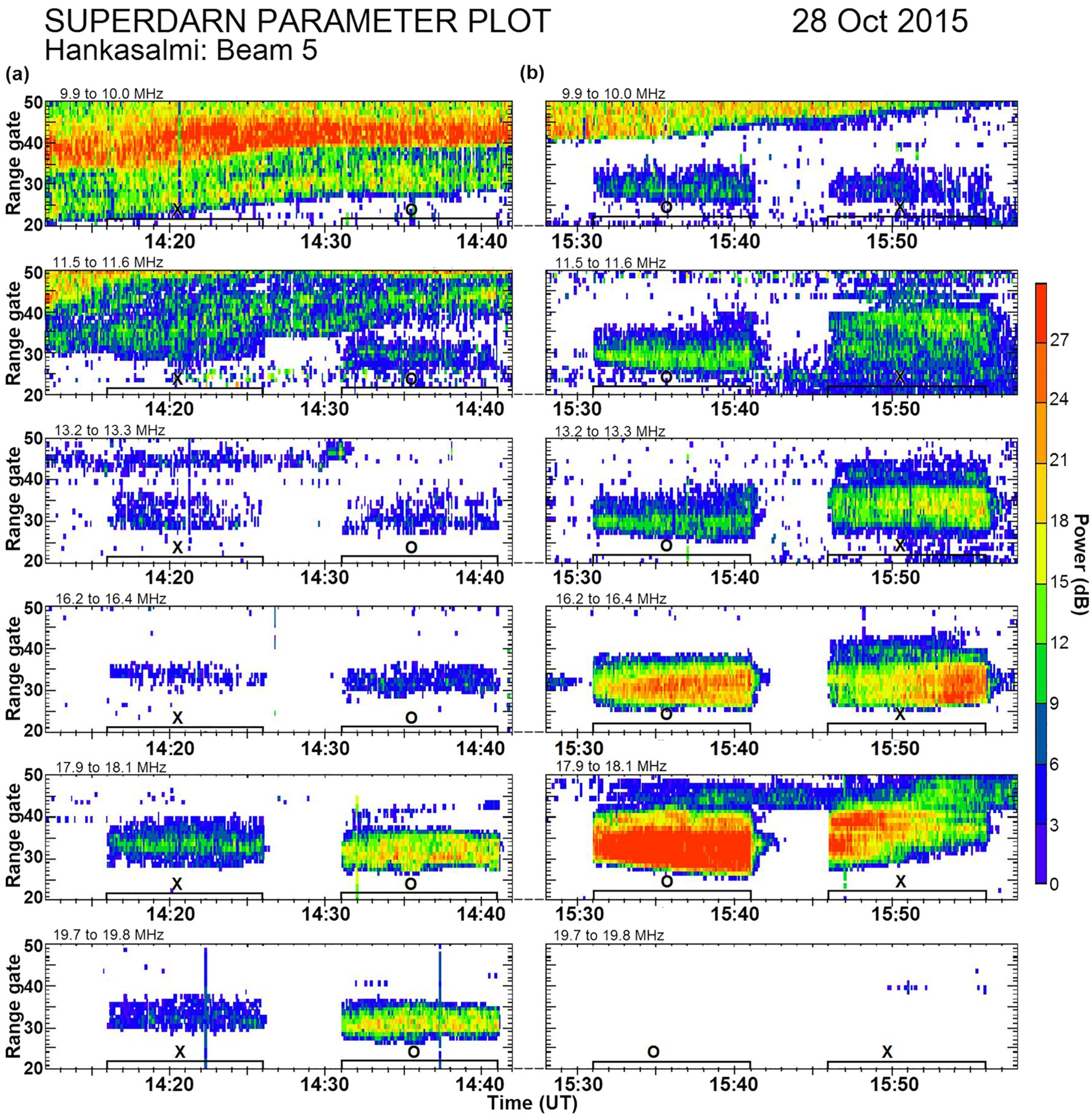

Figure 7. Experiment 2. The backscatter power from Co-operative UK Twin Located Auroral Sounding System (CUTLASS) Finland (SuperDARN) radar observations (beam 5) at operational frequencies of 10, 11.5, 13.2, 16, 18, and 20 MHz depending on the range gate and time in the course of O- and X-mode pumping on October 28, 2015. (a) High frequency (HF) pumping at $f_H = 6.77$ MHz from 14:12–14:42 UT. (b) HF pumping at $f_H = 5.423$ MHz from 15:28–15:53 UT. The pump pulses and polarization of the heater wave are shown on the time axis. The heater details are the same as in Figure 4.

recorded far away from the EISCAT/Heating facility, occurred only in the course of X-mode HF pumping. Thus, during O-mode pulse the full O-mode effective radiated power (ERP = 240–480 MW) was not able to excite any ion gyro-harmonic discrete structures in the NSEE spectra. Because of that it is quite clear that

Figure 6. Experiment 2. The power spectra of narrowband stimulated electromagnetic emission (NSEE) on October 28, 2015 at $f_H = 5.423$ MHz in the frequency band of ±250 Hz taken over 3 s intervals in the course of the X-mode pulse from 15:46 to 15:56 UT. Digits on the X-mode spectrum taken at 15:46:15–15:46:18 UT indicate the frequency offsets of the observed downshifted and upshifted spectral maxima. There are also spectral maxima, most pronounced in the downshifted sideband, corresponding to the values of $0.5f_{ci}$ and even $1.5f_{ci}$ for O^+ ions. Such spectral maxima correspond approximately to the ion gyro-frequency for NO^+ ions and its third harmonic. The heater details are the same as in Figure 4.

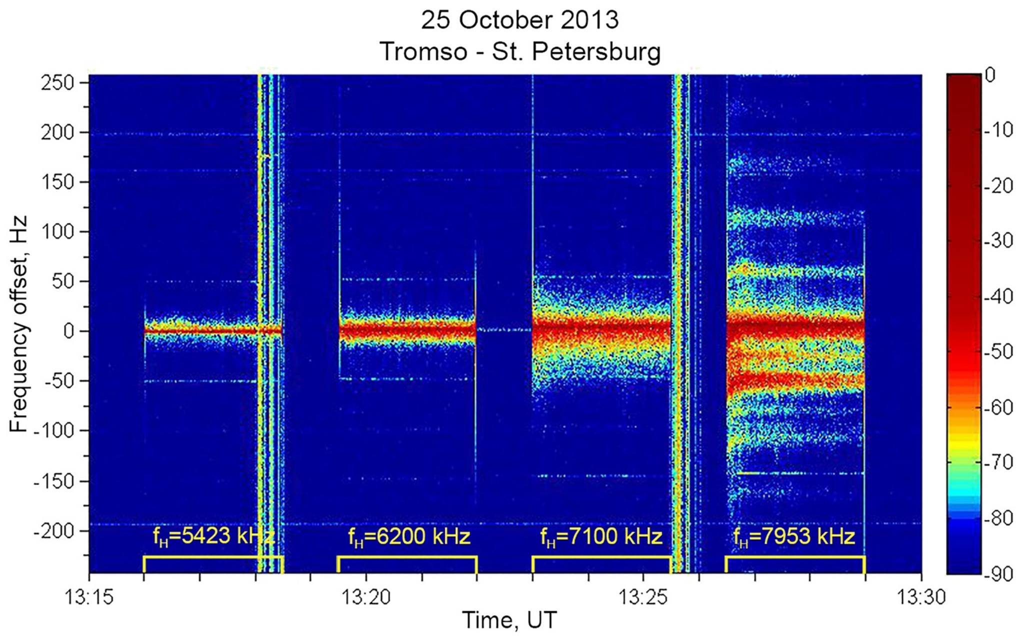

Figure 8. Experiment 3. The spectrogram of the narrowband stimulated electromagnetic emission (NSEE) in the frequency band of ±250 Hz off the pump frequency taken on October 25, 2013 from 13:15 to 13;30 UT obtained near St. Petersburg at 1,200 km away the EISCAT/Heating facility. An extraordinary polarized high frequency (HF) pump wave radiated from 13:16 UT at frequencies of 5.423, 6.2, 7.1 and 7.953 MHz with the effective radiated power of ERP = 416, 548, 615, and 740 MW respectively with a 2.5 min on, 1 min off transmission scheme. The pump pulses and pump frequencies are shown on the time axis.

the small part of the O-mode ERP (leakage of the O-mode) cannot certainly excite the spectral structures in the course of the X-mode HF pumping. On the other side, the leakage of the X-mode pump wave in the course of the O-mode pump pulse was not able to generate the ion gyro-harmonic structures. It means that the threshold of the excitation of the ion gyro-harmonic structures was higher than the X-mode leakage. Observations of the of X-mode ion gyro-harmonic structures in the NSEE spectra far away from the Heating facility provide new capabilities of investigations of the nonlinear plasma processes, producing NSEE, which are not realised under O-mode HF pumping in the close vicinity of the HF Heating facility.

Below we summarize the main features of the discrete spectral structures within ±1 kHz off the heater frequency observed under X-mode HF pumping. They were ordered by approximately the ion gyro-frequency for O^+ ions and observed simultaneously in the downshifted and upshifted sidebands of the NSEE spectra.

Multiple ion gyro-harmonic structures with the maximum spectral power at nf_{ci}, where n is the harmonic number, can be recognized in the spectrograms. As observations considered here have shown, the number of ion gyro-harmonic structures depends on the proximity of the HF pump wave to the electron gyro-harmonic frequencies and the ratio of the pump frequency to the critical frequency of the $F2$ layer. The intensity of the first downshifted spectral peak was below the pump wave power by 15–30 dB and maximized in the frequency offset range of −(53.4–58.8) Hz in different experiments, while the power of the first upshifted ion gyro-harmonic structure was less than the pump wave power by 30–40 dB and peaked at +(51.1–56.3) Hz, that is just less than the first downshifted spectral maximum. With increase of the harmonic number the intensity of down- and upshifted spectral peaks gradually decayed and the spectral width of the discrete structures increased from 20 to 50 Hz, the latter is about the ion gyro-frequency f_{ci} for O^+ ions. This leads us to believe that the generation of the ion gyro-harmonic structures is most likely a cascading process. As was shown by Samimi et al. (2013), more ion gyro-harmonic lines are typically associated with more electron acceleration perpendicular to the geomagnetic field.

There are, in addition, downshifted spectral lines at $0.5f_{ci}$ and occasionally even at $1.5f_{ci}$, where f_{ci} is the ion gyro-frequency for O^+ ions. The downshifted components at $0.5f_{ci}$ and $1.5f_{ci}$ can be paired with less pro-

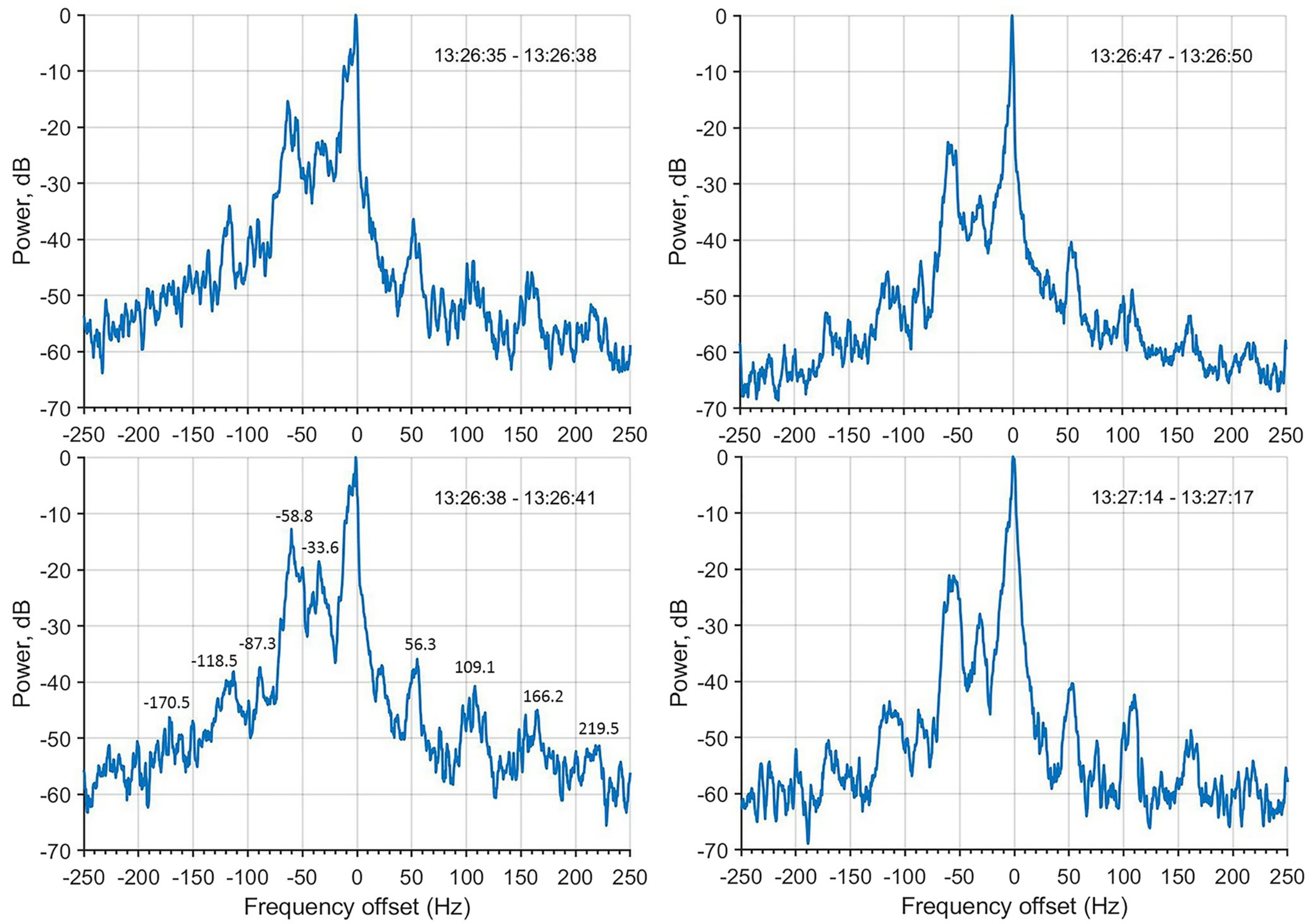

Figure 9. Experiment 3. The power spectra of narrowband stimulated electromagnetic emission (NSEE) on October 25, 2013 at f_H = 7.953 MH in the frequency band of ±250 Hz taken over 3 s intervals in the course of the X-mode pulse from 13:26:30 to 13:29 UT. Digits on the spectrum taken at 13: 26:38–13:26:41 UT indicate the frequency offsets of the observed downshifted and upshifted spectral maxima which are close to the harmonics of the ion gyro-frequency for O^+ ions. There are also spectral maxima, most pronounced in the downshifted sideband, corresponding to the values of 0.5 f_{ci} and even 1.5 f_{ci} for O^+ ions. Such spectral maxima correspond approximately to the ion gyro-frequency for NO^+ ions and its third harmonic. The heater details are given in Figure 8.

nounced upshifted spectral lines. The spectral structure at 0.5 f_{ci} peaked at frequency offsets about -(28.5–33) Hz. Actually, the reflection altitude of the X-mode pump wave varied between 212 and 230 km at different sets of experiments. The most intense downshifted structures at 0.5f_{ci} and 1.5f_{ci} paired with the upshifted lines were generated at the lowest reflection altitude of 212–222 km (on October 28, 2013 at f_H = 7.953 MHz, see Figure 8). At higher reflection heights of 220–230 km (on February 25, 2013 at f_H = 5.423 MHz and on October 28, 2015 at f_H = 6.77 MHz, see Figures 1 and 4 accordingly) only downshifted spectral emissions at ∼ 0.5 f_{ci} were observed in the NSEE spectra.

The observed frequency offset corresponds approximately to the ion gyro-frequency for NO^+ ions. From the IGRF model the ion gyro-harmonic frequency for NO^+ ions is estimated to be 24.87–24.95 Hz in different sets of experiments. They can provide the essential input at altitudes of 200–220 km. This leads us to suggest that the spectral structures, maximized at the frequency offset of (28.5–33) Hz, may be related to the ion gyro-frequency for NO^+ ions. These emission lines should be more pronounced at lower altitudes as observed in our experiments. Moreover, as was shown by Bernhardt et al. (2010), upshifted emission lines are expected to be weaker than downshifted spectral lines. As a consequence, at high reflection altitudes the intensity of upshifted spectral lines for NO^+ ions may drop below the noise level. It should be also noted that the ion gyro-frequency for NO^+ ions is slightly higher than the value of 0.5 f_{ci} for O^+ ions. The same was observed in our experiments, that is another argument in support of the generation the ion gyro-frequency for NO^+ ions.

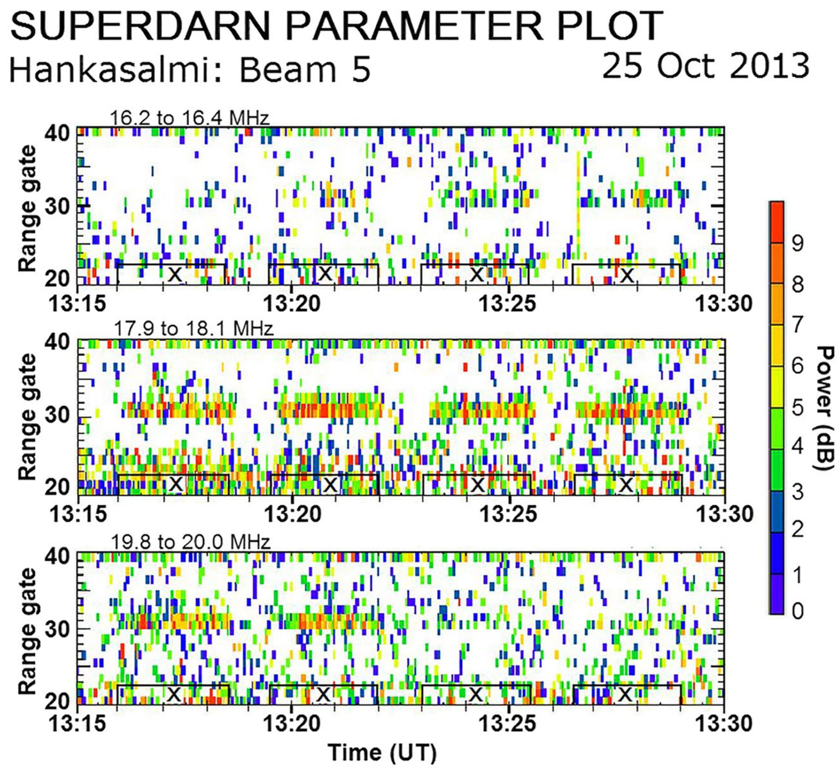

Figure 10. Experiment 3. The backscatter power from Co-operative UK Twin Located Auroral Sounding System (CUTLASS) Finland (SuperDARN) radar observations (beam 5) at operational frequencies of about 16, 18, and 20 MHz depending on the range gate and time in the course of X-mode pumping on October 25, 2013 from 13:15 to 13:30 UT. The pump frequencies and heater details are the same as in Figure 8. The pump pulses are shown on the time axis.

As evident from the CUTLASS observations, both X- and O-mode pump pulses were accompanied by FAI generation (see Figure 7). However, the occurrence of the discrete ion gyro-harmonic structures in the NSEE spectra, recorded at a distance of 1,200 km from Tromsø, was only observed in the course of the X-mode HF pumping.

The ion gyro-harmonic structures start to appear 5–15 s after the X-mode pumping onset. It was found that the temporal evolution of the ion gyro-harmonic structures depends on the preconditioning effects. Comparing two consecutive the X-mode pulses, it is seen that from the "cold" start the ion gyro-harmonic structures appeared ~5 s after the heater is turned on, while in the next X-mode pulse they already developed after 5 s (see Figures 1 and 2). Thus, the results obtained make it clear that the temporal evolution of the ion gyro-harmonic structures, induced by an X-mode HF pumping, depends on the preconditioning effects.

Our observational results have clearly demonstrated that multiple ion gyro-harmonic structures, observed at a large distance from the EISCAT/Heating facility, were only recorded with X-mode HF pumping. Let's consider the observational results of the emission lines in the NSEE spectra in the vicinity of EISCAT/Heating facility. Until the present time the NSEE observations with an X-mode HF pump wave have not been carried out near the EISCAT/Heating facility. However, in the HAARP experiments the NSEE observations were all done in the vicinity of the HF heater, and in none of the HAARP experiments were excited IA and EIC lines observed during X-mode HF pumping (Mahmoudian, Scales, Bernhardt, Fu, et al., 2013; Mahmoudian et al., 2014). As for O-mode HF pumping at the EISCAT site, Borisova et al. (2014) have analyzed in detail results from multi-instrument observations, including NSEE measurements, during frequency stepping experiments in the vicinity of the fourth electron gyro-harmonic, 4*f*ce. These experiments, similar to our alternating O-/X-mode experiments below 4*f*ce, have been carried out at pump frequencies just below the critical frequency of the F2 layer ($f_H/\,foF2 \le 1$). Down- and upshifted structures in the NSEE spectra, corresponding to the IA plasma waves, were observed at pump frequencies below and above the forth electron gyro-harmonic and disappeared as the pump frequency approached close to 4*f*ce. They were accompanied by intense FAIs and the downshifted maximum (DM) component in the wideband SEE (WSEE) spectra. Multiple ion gyro-harmonic discrete spectral structures were not observed in the NSEE spectra recorded near the EISCAT/Heating facility.

What is the generation mechanism for the discrete ion gyro-harmonic structures induced by the X-mode HF pumping? There is some analogy between discrete spectral structures ordered by the ion gyro-frequency (for O $^{+}$ions) observed under X-mode HF pumping at a distance of 1,200 km from EISCAT/Heating at Tromsø and structures recorded at the HAARP facility under O-mode heating in the vicinity of the second harmonics of the electron gyro-frequency (Bernhardt et al., 2011; H. Fu et al., 2013; Mahmoudian, Scales, Bernhardt, Samimi, et al., 2013; Samimi et al., 2012, 2013, 2014). Samimi et al. (2013) proposed that the generation mechanism of the downshifted discrete spectral structures ordered by the ion gyro-harmonic frequency was via parametric decay of the pump electromagnetic field into an upper hybrid/or electron Bernstein wave and neutralized ion Bernstein modes SIBS.

Despite that the ion gyro-harmonic structures, generated by the X-mode HF pump wave at frequencies below the electron gyro-harmonics, have some similarity with the O-mode ion gyro-harmonic structures observed at HAARP, there are significant distinctions between them.

First of all, at HAARP the observed structures were only downshifted from the heater frequency and the maximum spectral power occurred for $(n + 0.5)f_{ci}$, where n is the harmonic number. In our X-mode experiments, the downshifted (Stokes) spectral lines were paired with upshifted (anti-Stokes) spectral lines. In addition, the spectral maxima were observed for nf_{ci}, where f_{ci} is the ion gyro-harmonic frequency for O^+ ions and n is the number of harmonic.

Under O-mode HF pumping at HAARP all spectral discrete structures start to develop at the same time, suggesting simultaneous excitation rather than a nonlinear cascading process (Samimi et al., 2013). A nonlinear cascading process is most likely to occur in the course of the X-mode HF pumping. It was especially pronounced on February 25, 2013 in the first X-mode pulse from 16:16 to 16:26 UT (see Figure 1), when the X-mode pump wave was radiated below the fourth electron gyro-harmonic.

Moreover, the generation mechanism of stimulated spectral lines in the NSEE spectra cannot principally be the same for the O- and X-mode pump waves. This is evident from alternating O/X-mode pumping when the discrete spectral structures were observed at a large distance from the EISCAT/Heating facility (1,200 km) only for X-mode pulses in spite of FAIs being generated both for O- and X-mode heating.

We assume that discrete spectral structures (within ±1 kHz off the heater frequency), generated by an X-mode HF pump wave and observed at a large distance (1,200 km) from the EISCAT/Heating, have a connection with a MSBS process, when the powerful electromagnetic wave directly decays into the low frequency electrostatic decay mode and a backscattered electromagnetic wave. As was shown by Bernhardt et al. (2010) in previous observations of the MSBS spectral structure, the low frequency decay mode is an EIC wave.

As we have shown, the downshifted and upshifted EIC harmonic waves were generated below the fourth, fifth, and sixth electron gyro-harmonic frequencies. We suggest, that in such a case a multiple MSBS process can be realized. At first the X-mode powerful electromagnetic wave (EM_0) at the reflection altitude directly decays into an EIC wave and a backscattered electromagnetic wave (EM), $EM_0 \rightarrow EIC_1 + EM_1$. EIC harmonic waves are generated due to next decays as follows:

$$\begin{aligned} EM_1 &\rightarrow EIC_2 + EM_2, \\ EM_2 &\rightarrow EIC_3 + EM_3, \text{etc.} \end{aligned}$$

We suggest that the region in which the MSBS process developed is the reflection altitude of the extraordinary polarized HF pump wave, having the wave vector and electric field perpendicular to the magnetic field. Therefore, under X-mode HF pumping toward MZ the wave vectors of the EIC and backscattered electromagnetic waves, similar to the wave vector of the X-mode wave, are perpendicular to B in the interaction region. We believe that backscattered electromagnetic waves are scattered from FAIs in the direction perpendicular to B and are able to propagate to a large distance from the heating facility. On the other hand, the orientation of the wave vectors of the EIC and backscattered EM wave in the source region is precluiding seeing the same emission lines from a location close to the heating facility.

Besides the direct conversion of the extraordinary polarized electromagnetic pump wave (EM) into an EIC wave and a backscattered electromagnetic wave, we cannot rule out the possibility of the indirect conversion of the X-mode EM wave. The wave vector of such EM wave, radiated toward the magnetic zenith, is perpendicular to the background magnetic field near the reflection altitude. Here an X-mode EM wave may decay into HF electron Bernstein wave and low frequency ion Bernstein wave, EM → EB + IB (Sharma et al., 1994). We assume that this "mother" EB wave can further decay into newly generated "daughter" EB wave and ion Bernstein wave, EB → EB_1 + IB_1. Next decays can also occur. In such a case a nonlinear cascading process is developing, that leads to the excitation of discrete spectral structures ordered by the ion gyro-frequency for O^+ ions through the SIBS process. As was shown by Samimi et al. (2014), the excitation of a larger number of the ion Bernstein modes is associated with more electron acceleration perpendicular to the geomagnetic field. FAIs play a key role for the NSEE occurrence at a large distance from the EISCAT/Heating. The NSEE received on the ground is an electromagnetic wave generated in the source region near the reflection altitude, while the HF decay modes are electrostatic EB waves. Thus, these electrostatic waves should certainly convert back to the downward propagating electromagnetic waves. The HF electrostatic waves (EB) with the wave vector perpendicular to the magnetic field B, are scattered from field-aligned irregularities in the direction perpendicular to B and convert back into an EM wave which can be received on the ground.

As evident from CUTLASS observations, in the course of experiments FAIs were generated by X- and O-mode waves both. The radical difference between O- and X-mode pump wave near the reflection level is the direction of the wave vector relatively to the magnetic field, $k_o \parallel B$ for O-mode and $k_x \perp B$ for X-mode respectively. In accordance with the theoretical predictions (Bernhardt et al., 2010; Shukla & Stenflo, 2010), the IA waves are excited when the wave vector in the interaction region pointed along the magnetic field B, that in our experiments is realized for an O-mode pump wave. The EIC or IB waves are dominant nearly perpendicular to B that is realized in the course of X-mode HF pumping toward the magnetic zenith.

Therefore, the O- and X-mode HF pump waves radiated toward MZ excite different types of electrostatic waves – either IA, which are parallel to B, or EIC or IB which are perpendicular to B. As was shown by H. Y. Fu et al. (2020) and Borisova et al. (2014), in the course of EISCAT experiments toward MZ with the O-mode pumping only IA emission lines were observed in the NSEE spectra which were recorded in the close vicinity of EISCAT/Heating facility. In this connection we suggest that in our O-mode experiments IA waves can be excited near the reflection altitude. However, when the wave vectors of the IA and backscattered electromagnetic waves are parallel to B, these waves are not able to be scattered from FAIs in the direction perpendicular to B and observed at a large distance from EISCAT/Heating facility.

By a contrast, in the course of the X-mode HF pumping toward MZ the ion gyro-harmonic structures (for O^+ ions) and their multiple harmonics were observed in the NSEE spectra which were received at a large distance of 1,200 km far away from the EISCAT/Heating facility. We suggest that EIC or IB emission lines in NSEE spectra can be recorded on the ground at a distance from the interaction region up to ∼1,500–1,700 km which corresponds to half of the length of one-hop propagation for the F2 layer due to scattering in the direction perpendicular to B.

We have considered the MSBS and SIBS as relevant processes for the observed multiple down- and upshifted ion gyro-harmonic structures in the NSEE spectra. For choosing the preferential mechanism for the excitation of multiple ion gyro-harmonic structures, induced by an X-mode HF pumping toward MZ, the theoretical investigations and more experiments are called for.

Figure 11 presents the EISCAT UHF incoherent scatter radar (run at 933 MHz) observations of the electron density N_e, of electron temperature T_e, raw electron density (backscattered power), and undecoded plasma lines in the course of the first set of experiments on February 25, 2013. The EISCAT UHF radar data were processed with 30 s integration time by using the Grand Unified Incoherent Scatter Design and Analysis Package software (Guisdap) (Lehtinen & Huuskonen, 1996). The EISCAT UHF radar, co-located with the HF heating facility, provides direct observations of HF-induced plasma waves with near field-aligned propagation, Powerful electromagnetic wave (pump wave) decays into HF-induced Langmuir (L) wave and

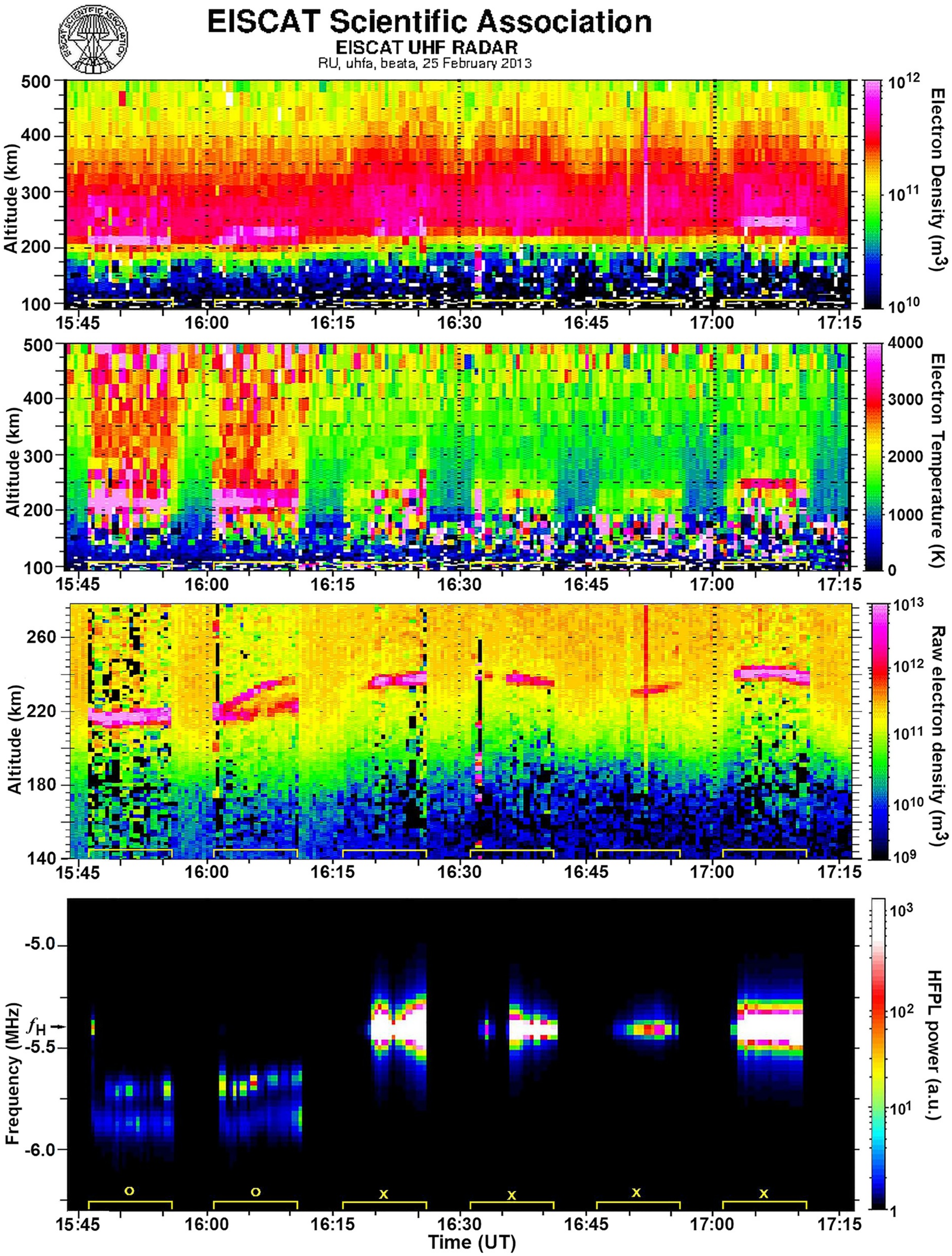
EISCAT Scientific Association
EISCAT UHF RADAR
RU, uhfa, beata, 25 February 2013
Altitude (km)
Electron Density (m3)
Electron Temperature (K)
Raw electron density (m3)
Frequency (MHz)
HFPL power (a.u.)
Time (UT)
15:45
16:00
16:15
16:30
16:45
17:00
17:15
fH
o
x

Figure 11.

HF-enhanced IA wave in the vicinity of the reflection altitude of the HF pump wave (Hagfors et al., 1983; Robinson, 1989). In the UHF radar spectra they appear as HF-induced plasma lines in the high-frequency measurement channel and HF-enhanced ion lines in the low-frequency measurement channel.

From Figure 11 it is clearly seen that strong electron temperature increases were observed in the first two O-mode pulses (15:46–15:56 and 16:01–16:11 UT). The N_e behavior did not exhibit significant changes as compared with the background values. It should be noted, that intense backscattered power from UHF radar measurements, corresponding to the excitation of the IA waves near the reflection altitude of the pump wave, prevents the correct estimation of N_e and T_e at the same altitudes. Because of that, we did not use the altitude range of 200–250 km for N_e and T_e estimations. As evident from Figure 11, strong T_e increases were coexisting with the excitation of HF-induced ion -acoustic and plasma waves. Interesting behavior of the O-mode plasma lines was observed. After an initial overshoot, excited as an immediate response to the heater turn-on, two outshifted plasma lines, excited at the heater frequency close to foF2 and below $4f_{ce}$ were observed in the course of O-mode pumping. As was shown by Borisova et al. (2019), two spectral maxima outshifted in frequency with respect to the pump frequency by $\Delta_1 \approx 0.19–0.28$ MHz and $\Delta_2 \approx 0.30–0.45$ MHz were observed at the altitudes of the upper-hybrid resonance and at the reflection altitudes of the pump wave, respectively. The excitation of the plasma line outshifted by 0.30–0.45 MHz was explained by the dispersion properties of the Langmuir wave in a plasma with allowance for the finite electron temperature (free mode) (see, for example, DuBois et al., 1993; Mishin et al., 1997; Rietveld et al., 2000). The excitation of plasma lines outshifted by 0.19–0.28 MHz was explained by the interaction of Bernstein waves, ionospheric plasma waves, and upper-hybrid waves excited due to the pump-wave transformation (Borisova et al., 2019).

By a contrast, during X-mode pumping the T_e increases were not too large and did not exceed 30% above the background level. HF-induced plasma and ion lines were generated through the whole pump pulses, but outshifted plasma lines were not excited in the course of X-mode heating. The typical feature of the experiment on February 25, 2013, similar to a large number of other X-mode experiments (Blagoveshchenskaya et al., 2011, 2013, 2014, 2015, 2020), is a strong N_e enhancement in a wide altitude range, observed only in a magnetic field-aligned direction for all X-mode pulses (see Figure 11). Such N_e increases can be produced by electron acceleration, as was found by Carlson et al. (1982, 2016). Moreover, the acceleration of electrons along the magnetic field line in the course of X-mode HF pumping is also confirmed by the excitation of strong optical emission in the red and green lines and high ratio of intensities of green to red line (Blagoveshchenskaya et al., 2014).

Comparing the NSEE and EISCAT UHF radar observational results, we conclude that the electron accelerations along and across the magnetic field coexist during X-mode heating at pump frequencies below the fourth, fifth and sixth electron gyro-harmonics

We have shown that an HF pump wave with an extraordinary polarization (X-mode), radiated into the F region of the high latitude ionosphere in the magnetic zenith direction at frequencies below the fourth, fifth, and sixth electron gyro-harmonics, is able to excite multiple downshifted discrete ion gyro-harmonic structures paired with the upshifted spectral components (Stokes and anti-Stokes modes) in the NSEE spectra within ±1 kHz around the pump frequency. They coexisted with FAIs and were recorded at a large distance (1,200 km) away from EISCAT/Heating. We suggest that the observed spectral structures ordered by the ion gyro-frequency have a connection with MSBS process, when the HF pump wave directly decays into the ion gyro-harmonic and a backscattered electromagnetic wave. There are a number of unanswered questions about the NSEE spectral features and more experiments are required. It is necessary to investigate in more detail the features of the X-mode NSEE spectra in the close vicinity of the Heating facility and to compare them with the O-mode spectral features, as well as with the X-mode NSEE spectral components observed far away from the Heating facility. Theoretical investigations for choosing the preferential mechanism for the excitation of multiple ion gyro-harmonic structures induced by an X-mode pump wave and more experiments are called for. Taking into account that X-mode phenomena are excited when the pump frequency is

Figure 11. Experiment 1. Temporal variations of the electron density N_e, electron temperature T_e, raw electron density (backscattered power), and powers of the undecoded plasma lines from the EISCAT UHF radar measurements with 30 s integration time in the course of the first set of experiments at $f_H = 5.423$ MHz on February 25, 2013 from 15:45 to 17:15 UT. The correct estimations of N_e and T_e cannot be obtained in the altitude range of 200–250 km due to intense backscattered power, corresponding to the excitation of the IA waves near the reflection altitude of the pump wave. The heater details are the same as in Figure 1. The pump pulses and polarization of the heater wave are shown on the time axis.

below as well above the critical frequency ($f_H \leq foF2$ and $f_H > foF2$) (Blagoveshchenskaya et al., 2015, 2019), we plan to investigate the X-mode spectral structures under $f_H > foF2$ and their connection with FAIs in future. The excitation threshold for X-mode discrete spectral structures in the NSEE spectra also remains an open question.

Conflict of Interest

The authors declare no conflicts of interest relevant to this study.

Data Availability Statement

The data supporting the conclusions can be obtained through EISCAT Madrigal database (https://portal.eiscat.se/madrigal/) and the AARI database (http://www.geophys.aari.ru/heating/).

Acknowledgments
EISCAT is an international scientific association supported by research organizations in China (CRIRP), Finland (SA), Japan (NIPR and STEL), Norway (NFR), Sweden (VR), and the United Kingdom (NERC). The authors acknowledge the use of SuperDARN data. SuperDARN is a collection of radars funded by the national scientific funding agencies of Australia, Canada, China, France, Italy, Japan, Norway, South Africa, the United Kingdom, and the United States. The authors are thankful to Dr. M. Rietveld for the calculations of effective radiated powers under O- and X-mode HF pumping. The authors are also grateful to the reviewers for useful comments. N F. Blagoveshchenskaya, T D. Borisova, and A S. Kalishin are supported by the Arctic and Antarctic Research Institute. T K. Yeoman is supported by Science and Technology Facilities Council Grant ST/H002480/1.

References

Bernhardt, P. A., Selcher, C. A., & Kowtha, S. (2011). Electron and ion Bernstein waves excited in the ionosphere by high power EM waves at the second harmonic of the electron cyclotron frequency. *Geophysical Research Letters*, *38*, L19107. https://doi.org/10.1029/2011GL049390

Bernhardt, P. A., Selcher, C. A., Lehmberg, R. H., Rodriguez, S. P., Thomason, J. F., Groves, K. M., et al. (2010). Stimulated Brillouin Scatter in a magnetized ionospheric plasma. *Physics Review Letters*, *104*, 165004. https://doi.org/10.1103/PhysRevLett.104.165004

Bernhardt, P. A., Selcher, C. A., Lehmberg, R. H., Rodriguez, S. P., Thomason, J. F., McCarrick, M. J., & Frazer, G. J. (2009). Determination of the electron temperature in the modified ionosphere over HAARP using the HF pumped Stimulated Brillouin Scatter (SBS) emission lines. *Annales Geophysicae*, *27*, 4409–4427. https://doi.org/10.5194/angeo-27-4409-2009

Blagoveshchenskaya, N. F. (2020). Perturbing the high-latitude upper ionosphere (F region) with powerful HF radio waves: A 25-year collaboration with EISCAT. *URSI Radio Science Bulletin*, *373*, 40–55. https://doi.org/10.23919/URSIRSB.2020.9318436

Blagoveshchenskaya, N. F., Borisova, T. D., Kalishin, A. S., Yeoman, T. K., & Häggström, I. (2017). First observations of electron gyro-harmonic effects under X-mode HF pumping the high latitude ionospheric F-region. *Journal of Atmospheric and Solar-Terrestrial Physics*, *155*, 36–49. https://doi.org/10.1016/j.jastp.2017.02.003

Blagoveshchenskaya, N. F., Borisova, T. D., Kalishin, A. S., Yeoman, T. K., & Häggström, I. (2020). Distinctive features of Langmuir and Ion-acoustic Turbulences induced by O- and X-mode HF Pumping at EISCAT. *Journal of Geophysical Research: Space Physics*, *125*, e2020JA028203. https://doi.org/10.1029/2020JA028203

Blagoveshchenskaya, N. F., Borisova, T. D., Kalishin, A. S., Yeoman, T. K., Schmelev, Y. A., & Leonenko, E. E. (2019). Characterization of artificial, small-scale, ionospheric irregularities in the high-latitude *F* region induced by high-power, high-frequency radio waves of extraordinary polarization. *Geomagnetism and Aeronomy*, *59*(6), 759–773. https://doi.org/10.1134/s0016793219060045

Blagoveshchenskaya, N. F., Borisova, T. D., Kosch, M., Sergienko, T., Brändström, U., Yeoman, T. K., & Häggström, I. (2014). Optical and ionospheric phenomena at EISCAT under continuous X-mode HF pumping. *Journal of Geophysical Research: Space Physics*, *119*, 10483–10498. https://doi.org/10.1002/2014JA020658

Blagoveshchenskaya, N. F., Borisova, T. D., Yeoman, T., Rietveld, M. T., Ivanova, I. M., & Baddeley, L. J. (2011). Artificial field-aligned irregularities in the high-latitude F region of the ionosphere induced by an X-mode HF heater wave. *Geophysical Research Letters*, *38*, L08802. https://doi.org/10.1029/2011GL046724

Blagoveshchenskaya, N. F., Borisova, T. D., Yeoman, T. K., Häggström, I., & Kalishin, A. S. (2015). Modification of the high latitude ionosphere F region by X-mode powerful HF radio waves: Experimental results from multi-instrument diagnostics. *Journal of Atmospheric and Solar-Terrestrial Physics*, *135*, 50–63. https://doi.org/10.1016/j.jastp.2015.10.009

Blagoveshchenskaya, N. F., Borisova, T. D., Yeoman, T. K., Rietveld, M. T., Häggström, I., & Ivanova, I. M. (2013). Plasma modifications induced by an X-mode HF heater wave in the high latitude F region of the ionosphere. *Journal of Atmospheric and Solar-Terrestrial Physics*, *105–106*, 231–244.

Borisova, T. D., Blagoveshchenskaya, N. F., Kalishin, A. S., Kosch, M., Senior, A., Rietveld, M. T., et al. (2014). Phenomena in the high-latitude ionospheric F region induced by a HF heater wave at frequencies near the fourth electron gyroharmonic. *Radiophysics and Quantum Electronics*, *57*(1), 1–19. https://doi.org/10.1007/s11141-014-9489-6

Borisova, T. D., Blagoveshchenskaya, N. F., Rietveld, M. T., & Häggström, I. (2019). Outshifted plasma lines observed in heating experiments in the high-latitude ionosphere at pump frequencies near electron gyroharmonic. *Radiophysics and Quantum Electronics*, *61*(10), 722–740. https://doi.org/10.1007/s11141-019-09931-8

Carlson, H. C., Djuth, F. T., & Zhang, L. D. (2016). Creating space plasma from the ground. *Journal of Geophysical Research: Space Physics*, *122*, 978–999. https://doi.org/10.1002/2016JA023880

Carlson, H. C., Wickwar, V. B., & Mantas, G. P. (1982). Observations of fluxes of suprathermal electrons accelerated by HF excited instabilities. *Journal of Atmospheric and Solar-Terrestrial Physics*, *44*, 1089–1100. https://doi.org/10.1016/0021-9169(82)90020-4

DuBois, D. F., Hanssen, A., Rose, H. A., & Russell, D. (1993). Space and time distribution of HF excited Langmuir turbulence in the ionosphere: Comparison of theory and experiment. *Journal of Geophysical Research*, *98*, 17543–17567. https://doi.org/10.1029/93ja01469

Fu, H., Scales, W. A., Bernhardt, P. A., Samimi, A., Mahmoudian, A., Briczinski, S. J., & McCarrick, M. J. (2013). Stimulated Brillouin scatter and stimulated ion Bernstein scatter during electron gyroharmonic heating experiments. *Radio Science*, *48*, 607–616. https://doi.org/10.1002/2013RS005262

Fu, H. Y., Jiang, M. L., Wang, K. N., Wu, J., Li, Q. L., Rietveld, M. T., et al. (2020). Electron temperature inversion by stimulated brillouin scattering during electron gyro-harmonic heating at EISCAT. *Geophysical Research Letters*, *47*. https://doi.org/10.1029/2020GL089747

Galkin, I. A., Reinisch, B. W., Huang, X., Song, P., Foster, J., Mendillo, M., & Bilitza, D. (2008). A tribute to the ARTIST, in Radio Sounding and Plasma Physics. *AIP Conference Proceedings*, *974*, 34–38. https://doi.org/10.1063/1.2885029

Grach, S. M., & Trakhtengerts, V. Y. (1975). Parametric excitation of ionospheric irregularities extended along the magnetic field. *Radiophysics and Quantum Electronics*, *18*(9), 951–957. https://doi.org/10.1007/bf01038190

Gurevich, A. V. (2007). Nonlinear effects in the ionosphere. *Physics-Uspekhi*, *50*, 1091–1121. https://doi.org/10.1070/pu2007v050n11abeh006212

Hagfors, T., Kofman, W., Kopka, H., Stubbe, P., & Ijnen, T. (1983). Observations of enhanced plasma lines by EISCAT during heating experiments. *Radio Science*, *18*, 861–866. https://doi.org/10.1029/rs018i006p00861

Lehtinen, M. S., & Huuskonen, A. (1996). General incoherent scatter analysis and GUISDAP. *Journal of Atmospheric and Solar-Terrestrial Physics*, *58*, 435–452. https://doi.org/10.1016/0021-9169(95)00047-x

Lester, M., Chapman, P. J., Cowley, S. W. H., Crooks, S. J., Davies, J. A., Hamadyk, P., et al. (2004). Stereo CUTLASS: A new capability for the SuperDARN radars. *Annales Geophysicae*, *22*, 459–473. https://doi.org/10.5194/angeo-22-459-2004

Leyser, T. B. (2001). Stimulated electromagnetic emissions by high-frequency electromagnetic pumping of the ionospheric plasma. *Space Science Reviews*, *98*, 223–328. https://doi.org/10.1023/a:1013875603938

Mahmoudian, A., Scales, W. A., Bernhardt, P. A., Fu, H., Briczinski, S. J., & McCarrick, M. J. (2013). Investigation of ionospheric stimulated Brillouin scatter generated at pump frequencies near electron gyroharmonics. *Radio Science*, *48*, 685–697. https://doi.org/10.1002/2013RS005189

Mahmoudian, A., Scales, W. A., Bernhardt, P. A., Isham, B., Kendal, E., Briczinski, S. J., et al. (2014). Electron gyroharmonic effects on ionospheric stimulated Brillouin scatter. *Geophysical Research Letters*, *41*, 5710–5716. https://doi.org/10.1002/2014GL061050

Mahmoudian, A., Scales, W. A., Bernhardt, P. A., Samimi, A., Kendall, E., Ruohoniemi, J. M., et al. (2013). Ion gyro-harmonic structuring in the stimulated radiation spectrum and optical emissions during electron gyro-harmonic heating. *Journal of Geophysical Research: Space Physics*, *118*, 1270–1287. https://doi.org/10.1002/jgra.50167

Mishin, E., Hagfors, T., & Kofman, W. (1997). On origin of outshifted plasma lines during HF modification experiments. *Journal of Geophysical Research*, *102*, 27265–27269. https://doi.org/10.1029/97ja02448

Mishin, E., Watkins, B., Lehtinen, N., Eliasson, B., Pedersen, T., & Grach, S. (2016). Artificial ionospheric layers driven by high-frequency radiowaves: An assessment. *Journal of Geophysical Research: Space Physics*, *121*, 3497–3524. https://doi.org/10.1002/2015JA021823

Norin, L., Leyser, T. B., Nordblad, E., Thidé, B., & McCarrick, M. (2009). Unprecedentedly strong and narrow electromagnetic emissions stimulated by high-frequency radio waves in the ionosphere. *Physics Review Letters*, *102*, 065003. https://doi.org/10.1103/physrevlett.102.065003

Pedersen, T., Gustavsson, B., Mishin, E., Kendall, E., Mills, T., Carlson, H. C., & Snyder, A. L. (2010). Creation of artificial ionospheric layers using high-power HF waves. *Geophysical Research Letters*, *102*(37), L02106. https://doi.org/10.1029/2009GL041895

Pedersen, T., McCarrick, M., Reinisch, B., Watkins, B., Hamel, R., & Paznukhov, V. (2011). Production of artificial ionospheric layers by frequency sweeping near the 2nd gyroharmonic. *Annales Geophysicae*, *102*(29), 47–51. https://doi.org/10.5194/angeo-29-47-2011

Rietveld, M. T., Isham, B., Kohl, H., Hoz, C. L., & Hagfors, T. (2000). Measurements of HF-enhanced plasma and ion lines at EISCAT with high altitude resolution. *Journal of Geophysical Research*, *105*, 7429–7439. https://doi.org/10.1029/1999ja900476

Rietveld, M. T., Senior, A., Markkanen, J., & Westman, A. (2016). New capabilities of the upgraded EISCAT high-power HF facility. *Radio Science*, *51*(9), 1533–1546. https://doi.org/10.1002/2016RS006093

Rietveld, M. T., Wright, J. W., Zabotin, N., & &Pitteway, M. L. V. (2008). The Tromsø dynasonde. *Polar Science*, *2*, 55–71. https://doi.org/10.1016/j.polar.2008.02.001

Rishbeth, H., & van Eyken, T. (1993). EISCAT: Early history and the first ten years of operation. *Journal of Atmospheric and Solar-Terrestrial Physics*, *55*, 525–542. https://doi.org/10.1016/0021-9169(93)90002-g

Robinson, T. R. (1989). The heating of the high latitude ionosphere by high power radio waves. *Physics Reports*, *179*, 79–209. https://doi.org/10.1016/0370-1573(89)90005-7

Samimi, A., Scales, W. A., Bernhardt, P. A., Briczinski, S. J., & McCarrick, M. J. (2014). Ion gyroharmonic structures in stimulated radiation during second electron gyroharmonic heating: 2. Simulations. *Journal of Geophysical Research: Space Physics*, *119*, 462–478. https://doi.org/10.1002/2013JA019341

Samimi, A., Scales, W. A., Bernhardt, P. A., Briczinski, S. J., Selcher, C. A., & McCarrick, M. J. (2012). On ion gyro-harmonic structuring in the stimulated electromagnetic emission spectrum during second electron gyro-harmonic heating. *Annales Geophysicae*, *30*, 1587–1594. https://doi.org/10.5194/angeo-30-1587-2012

Samimi, A., Scales, W. A., Fu, H., BernhardtBriczinski, P. A. S. J., McCarrick, M. J., & McCarrick, M. J. (2013). Ion gyroharmonic structures in stimulated radiation during second electron gyroharmonic heating: 1. Theory. *Journal of Geophysical Research: Space Physics*, *118*, 502–514. https://doi.org/10.1029/2012JA018146

Sharma, R. P., Kumar, A., Kumar, R., & Tripathi, Y. K. (1994). Excitation of electron Bernstein and ion Bernstein waves by extraordinary electromagnetic pump: Kinetic theory. *Physics of Plasmas*, *1*(3), 522–527. https://doi.org/10.1063/1.870796

Shukla, P. K., & Stenflo, L. (2010). Stimulated Brillouin scattering of electromagnetic waves in magnetized plasmas. *Journal of Plasma Physics*, *76*, 853–855. https://doi.org/10.1017/s0022377810000504

Thidé, B., Derblom, H., Hedberg, A., Kopka, H., & Stubbe, P. (1983). Observations of stimulated electromagnetic emissions in ionospheric heating experiments. *Radio Science*, *18*(6), 851–859. https://doi.org/10.1029/RS018i006p00851

Thidé, B., Kopka, H., & Stubbe, P. (1982). Observations of stimulated scattering of a strong high frequency radio wave in the ionosphere. *Physics Review Letters*, *49*, 1561–1564. https://doi.org/10.1103/physrevlett.49.1561

Vas'kov, V. V., & Gurevich, A. V. (1976). Nonlinear resonance instability of plasma in the reflection region of ordinary electromagnetic wave. *Soviet Journal of Experimental and Theoretical Physics*, *42*(1), 91–97.